Response letter to Anonymous Referee #1

This study combines sea ice thickness retrievals from CryoSat-2 with different ice drift products to estimate the volume of ice export through the Fram Strait over the winters of 2010-2017. The authors find that ice drift variability dominates the variability of ice volume export over annual and inter-annual timescales, but the seasonal cycle is also impacted by the thickness of exported ice. The export of sea ice through the Fram Strait accounts for 54% of the variability of multiyear ice (MYI) volume over a given winter season.
The manuscript is clearly written and the figures are well-constructed and informative. Unfortunately, I still struggled with this review as I'm left wondering what the key pur- pose of the paper is. The manuscript includes a wealth of information but doesn't read like a complete method or scientific study. This is highlighted by the concluding bullets ranging from comparison of drift products to importance of ice export, presented as a list rather than a logical connected paragraph.
For a methods-based paper I would expect a more thorough description of the product development. This includes expansion on the error analysis explaining why the specific approach was chosen, how sea ice drift uncertainty is estimated using empirical error functions (brief summary of Sumata (2015) method), which high resolution SAR data is used a reference, and why such a reference is needed. The usefulness of the paper in a scientific sense is currently limited over such a short time frame, and it lacks novelty considering the number of existing sea ice export studies for the Fram Strait. The obvious way to develop the paper scientifically would be to investigate long-term trends in ice volume export, but as the authors state this would require a consistent methodology to compute ice volume flux through Fram Strait from multiple products.
I encourage the authors to think about their intended purpose for the paper then either a.) sufficiently describe the development of their new Arctic sea ice volume export product or b.) expand their scientific analysis utilizing the product. Despite these reservations I would like to repeat that this was a well-written paper and the content will be of interest to the sea ice community, so I have included some detailed and technical comments below.

We thank the reviewer for these thoughtful comments which helped to improve the paper. The novelty of the paper is to use the CryoSat-2 monthly ice thickness estimates for the computation of ice volume export. This hasn't been done before. Monthly retrievals allow a much more detailed analysis of the seasonal cycle and how the variabilities in sea-ice thickness, drift and concentration affect the volume export. These investigation were not (or very limited) possible with ICESat ice thickness retrievals that are available only twice per season (October-November and February-March), leaving gaps in December/January.
The Arctic research community is putting a lot of effort into quantifying contributions to exchanges between the Arctic and the North Atlantic (see ASOF for example, http://asof.awi.de). One key question is: What are the fluxes of mass, heat, liquid freshwater and ice from the Arctic Ocean into the subpolar North Atlantic (ASOF II Objectives)? Our study addresses some of these issues.
We have emphasized the scientific importance of this study in the revision. Nevertheless, we also included a more detailed description of the error estimates.

We have revised the paper substantially to address the comments from both reviews. The main changes are listed in the following:

- We have carefully revised the computation of the ice volume flux and checked the results.

- We have updated the NSIDC ice drift data set, since it is now available until February 2017, which allowed us to update the NSIDC ice volume export time series until the 2015/2016 season. 2016/2017 has not been computed, since March and April are still missing in the NSIDC data.

- The Methods section has been revised for a more detailed description of the ice volume export calculations, especially of the uncertainty estimates.

- We have added a figure showing the ice concentration along the Fram Strait Gate, corresponding to Figures 2 and 3 for sea ice thickness and sea ice drift.

- We have revised section 4.4, discussing the impact of openings in the MYI zone, which might lead to a positive bias in MYI growth rates due to erroneously classified MYI.

In the following, please find our responses separately for each of the detailed comments:

Detailed comments

P1L18-P2L7: The reasoning is not clear here with regards to concentrating on MYI and winter. For example, the authors should explicitly state that winter does not play such an important role for FYI mass balance, and why. They also mention summer ice concentration when the focus of the manuscript is on the winter period. If the authors want to justify their concentration on a given ice type and season then I suggest they first discuss winter ice mass balance variations (MYI and FYI) and then summer (MYI and FYI), then reach a logical conclusion.

In this paragraph, it is our intention to point on the importance of MYI for the Arctic ice mass balance and for the state of Arctic sea ice. Winter does indeed play an important role for FYI mass balance. However, in this study, we focus on the MYI export and its effect on MYI mass balance. We have revised this paragraph for clarification.

P2L16: State ICESat periods

We added the ICESat periods (October/November and February/March)

P2L20: “...we use the CS-2 ice thickness dataset...” -> “...we use *our* CS-2 ice thickness dataset. . .” There are numerous datasets, so the authors should be specific about which is used.

Agreed. We have added „AWI“ here.

P2L21: Be more explicit about which part of the study is novel (i.e. the “first” estimates of what). It is not the sea ice export estimates themselves, but the timeframe for which they’re provided.

The novel part is the time frame, but also, and even more, using CS-2 ice thickness data for the first time to estimate volume export rates. The CS-2 data allow for a much more detailed analysis of seasonal variability of ice volume export as it provides monthly estimates, in contrast to ICESat, which provided only two estimates per year. We have edited the introduction to emphasis the goals and the novelty of this paper.

P2L21: Define “winter”

We have added „(October-April)“ for clarification.

P4L21-23: Explain how unconstrained polynomials are dealt with at lower latitudes

Here, we consider the Warren climatology (W99) only in the Arctic Basin, e.g. where the polynomials are constraint by in situ measurements. For example, W99 shouldn’t be applied over Baffin Bay, or at least with caution.

P4L26: And also snow depth, correct?

Thank you, this is indeed missing here. Added.

P5L11-12: NSIDC products are also provided monthly

Added in the text.

P6 Figure 1: The FYI and MYI masks are quite hard to distinguish with the current color separation. I’d like to be able to see them clearly for each year.

We have enlarged the figures and slightly enhanced the contrast between the blue tones, so it should be easier to distinguish now.

P9 Figure 4: It is not clear why the frequency scale ranges from 0-25 for the right hand box. It's also hard to see the variation in the lines over one another. Sub-plots could work better here. It may be for thickness and drift the time-series isn't necessary, as the relevant data is already displayed in Figures 2 and 3.

We have changed this figure. Ice thickness, concentration and drift are now divided by their means for better comparison of their variability. The frequency refers to the number of samples that are within a given bin size of 0.2.

P9L7: "2012/2013" is repeated. I believe second date should be 2014/2015.

Thank you for pointing on this. The second date should have been 2013/2014. Corrected.

P12L5-6: I suggest moving the statement that the choice of drift product has no major impact on the variability analysis to the start of the start of the section, as until then I wasn't sure of the point of the section.

The point is that this statement is a result of the comparison between the different products. Therefore, we think that this statement should be somehow at the end of this section. However, we agree that the purpose of this comparison should be mentioned in the beginning. This has been added.

P14L1: Should this read "Similarly" rather than "On the other hand" as it's previously explained that uncertainty of ice drift also increases at lower latitudes.

This is true and we have exchanged "On the other hand" with „In addition".

P14L3: What is the "compromise" here? Uncertainty reduction vs. discarding higher ice velocities? It's not clear.

There is actually no compromise, therefore we changed this sentence to avoid confusion. In the western part, towards the coast of Greenland, the shelf area is more narrow than further south. Therefore, ice velocities are quite high also close to the coast, which might be associated with uncertainties in the low resolution drift product. On the other hand, further south, e.g. 80°N, the open ocean in the eastern part of the gate is associated with uncertainties in ice concentration and velocity as well. In any case, velocities at 82°N are more reliable than further south, as shown in Sumata et al. (2014).

P15L33: ". . .**seasonal** or **winter** MYI area loss can be explained almost entirely by ice export."

„winter" added.

Technical comments

P1 L1: "*Sea* ice volume export. . ."

Fixed.

P2L18: "sea-ice" -> "sea ice" for consistency

We have corrected this and avoided hyphenating throughout the paper.

P2L22: "access" -> "assess"

Fixed.

P3L11: "...(Continuous MCC)..." -> "...(Continuous Maximum cross-correlation (MCC)). . ."

Response letter to Anonymous Referee #2

The manuscript presents a new time series of Fram Strait sea ice volume export for the years 2010 to 2017. Fram Strait is the main gateway for sea ice leaving the Arctic and therefore estimates at that gate are a good indicator for sea ice mass change by ice export. The topic therefore is highly relevant for Arctic climate understanding. The authors describe a method solely based on satellite data, i.e., CryoSat-2 and microwave radiometer and scatterometer data. A similar method was applied before for different satellites but not for this combination and more recent years. While not discussed here the method potentially can serve as a tool to extend previous ice volume export time series. Results are discussed in connection with atmospheric forcing (NAO, AO) and the total Arctic mass balance. The topic is suitable for publication in The Cryosphere.
I, however, have some mayor concerns, which have to be addressed beforehand.

We thank the reviewer for these thoughtful comments which helped to improve the paper. We have revised the paper substantially to address the comments from both reviews. The main changes are listed in the following:

- We have carefully revised the computation of the ice volume flux and checked the results.

- We have updated the NSIDC ice drift data set, since it is now available until February 2017, which allowed us to update the NSIDC ice volume export time series until the 2015/2016 season. 2016/2017 has not been computed, since March and April are still missing in the NSIDC data.

- The Methods section has been revised for a more detailed description of the ice volume export calculations, especially of the uncertainty estimates.

- We have added a figure showing the ice concentration along the Fram Strait Gate, corresponding to Figures 2 and 3 for sea ice thickness and sea ice drift.

- We have revised section 4.4, discussing the impact of openings in the MYI zone, which might lead to a positive bias in MYI growth rates due to erroneously classified MYI.

In the following, please find our responses separately for each of your comment:

Mayor criticism:
- Flux calculations (eq. 2 & 3) seem to contain an error (varying length of grid cell not taken into account), which can cause the volume flux to be biased low by up to 40%. This has to be corrected or justified why the flux calculation is correct as it is given. This error will change the magnitude but not the variability of all calculation. Thus most conclusions will still be valid.

We took into account the varying length of the grid cell. In Eq. 2 and 3, the grid cell length l=25 km is divided by cos(lambda), where lambda represents the longitude. Therefore, the varying grid cell length is l_uv = l/cos(lambda). We have clarified this in the text.

- The Sea ice export estimates based on three different ice drift datasets do not agree within their uncertainty estimates. Which means that either the uncertainty estimates are wrong (to conservative) or some justification should be provided which dataset is more trustworthy. Otherwise the reader cannot use the information provided in a meaningful why. Unfortunately the difference is not just a bias but in some years exhibits different variability (Fig. 6b).

We applied the uncertainty estimation according to the drift error function given in Sumata et al. (2015). For a better understanding we have included the applied equations in the revised version of this paper. However, this drift error function does not contain biases or systematic errors. These have been investigated separately in Sumata et al. (2015). We have added a paragraph to better explain the error estimates and potential biases.

- Explanation of changes of MYI volume in the Arctic basin (4.4) does not sound physical to me. 4 out of 6 years show a gain of MYI ice volume through winter (100- 300km3/month), even after taking the ice export into account. The authors attribute that to thermodynamical growth. This would mean that in most cases ice growth for MY dominates the MYI ice volume change over ice export. I find that highly unlikely. The thermodynamic growth of snow covered MYI ice of >1.5m should be close to zero. Ice export through Fram Strait should by far dominate the month to month changes. The authors need to analysis this in more detail or provide more evidence. Actually, I assume their finding are dominated by the uncertainty of their MYI classification. They only use a binary MYI/FYI mask. The increase of MYI ice volume they observe could be well not MYI but FYI that growth in the leads or is otherwise integrated within the MYI within a 25 km grid cell. In summary, I don't think their conclusion that MYI volume is increasing in most months during winter is correct. Sea ice export should dominate the MYI volume change and cause it to be negative almost always.

We agree that section 4.4 was lacking a discussion of potential errors due to openings and forming of new ice within the MYI zone that are not well captured by the ice type product. This indeed contributes to the residual term in Eq. 5. Therefore, we have added a paragraph for clarification.
However, we are convinced that thermodynamic ice growth still plays a role for MYI. It is true that 2 m thick snow covered sea ice does not show relevant thermodynamic growth anymore, but thickness of second-year or third-year sea ice can decrease to 1 m during summer melt. Then, during the freeze-up, ice grows again, even if slowly, until it reached ~2 m. Buoy measurements from the Arctic Basin do capture this behavior (Figure R1). This buoy data set covers two freezing seasons from August 2013 to August 2015 and shows how thickness of second/third year sea ice decreased during summer melt and increases again during winter. To conclude, both effects (bias due to openings in the MYI zone + thermodynamic ice growth) most likely play a role and are therefore represented in Eq.5. It is difficult to separate the two effects since quantification is rather difficult and not within the scope of this study.

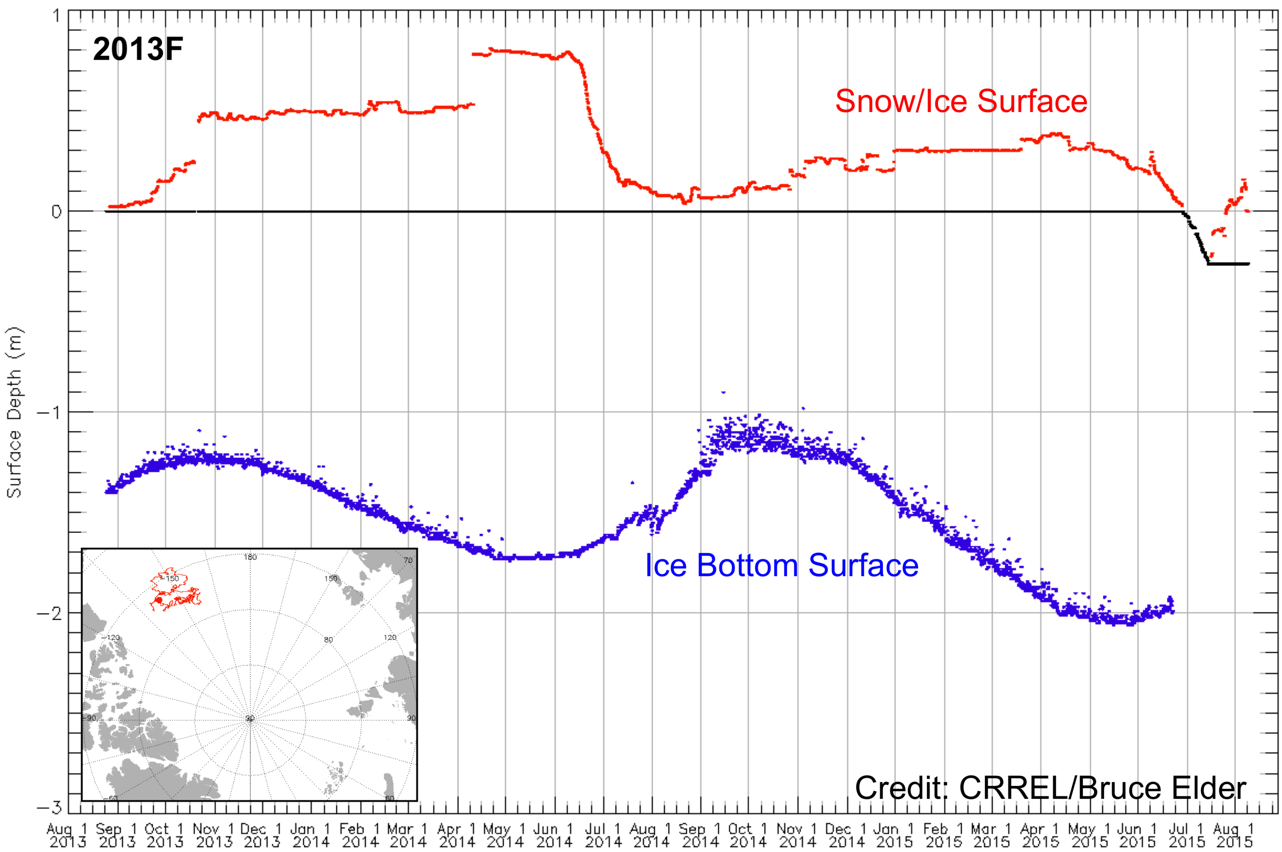

Figure R1: Snow/ice and bottom surface for ice mass balance buoy 2013F obtained from http://imb-crrel-dartmouth.org/imb.crrel/2013F.htm.

Detailed comments:

p1,l23: better split in two sentences. Sounds like the definition of MYI is connected to ice export.
Done. We also have restructured this part of the introduction.

p2,l1: add a sentence explaining how storms reduce sea ice.

We have added a sentence on this topic referencing a study by Parkinson et al., in which they have investigated the sea ice minimum in 2012.

p2,l4: "Multiple" you only name one.

Thank you for pointing that out. Corrected. We only refer to one study here.

p2,l13: what do you mean by "parametrization"? These studies were based on ULS ice thickness measurements.

„Parametrization" here means that thickness across Fram Strait is estimated using ULS ice thickness measurements from distinct locations in the Fram Strait.

p3, Table 1: the table should also include the name used for the three products in the text, i.e., OSISAF, IFREMER, NSIDC

Yes. Fixed.

p4/5, 2.3: Please discuss potential errors of MYI classification. You make quite strong use of the MYI dataset throughout this paper. However, in the convergent zone of Fram Strait, where ice gets deformed and broken up in smaller floes, ice type identification gets less reliable (surface scattering can dominate the volume scattering used for MYI type identification). Uncertainty estimates should be mentioned here and also more critically discussed later in the paper (e.g. in 3.1) when the ice types are analysed.

Thank you for pointing this out. The quantification of ice type errors is difficult because it might vary temporally and regionally, also depending on external factors. We have added paragraphs/ sentences in the relevant sections (2.3, 4.4) to discuss the uncertainties of the ice type products more carefully.

p5, l13: if you average them you wouldn't get the monthly displacement but the mean 48h displacement.

We agree that this formulation was misleading, and we have changed it.

p5, l19: hm, the gates are not aligned with the grid. The gates then would be not smooth lines like in the figure but step-wise functions, right? I think that makes flux calculations unnecessary complicated (see below). p5, eq. 2: why is l kept constant at 25km? Depending on the direction of the meridional or zonal component l can increase to sqrt(2)*l = 1.4*l=35km at 45◦ or not?

We calculate the export at the meridional (zonal) gate considering the line section crossing each grid cell. The length of the grid cell is thus a function of the longitude, which is considered in Eq. 2 as mentioned above. We have now changed the formulation and introduced l_uv = l/cos(lambda) to clarify this point.

p5, eq. 3: again, l should not be constant. With 40% the changes in effective length of your grid cell, which you did not take into account, could well dominate your error.

l/cos(lambda) does account for the changing length of the grid cell as a function of longitude. See above.

p6,l1 and ff: Do you apply the error functions from that paper to your datasets or do you use their values? Do these error values then vary in space and time? Shouldn't the error function depend on the drift dataset or dis Sumata evaluate all your three drift datasets? Please provide some more information and clearer description of method used here.

We do apply the error function from their paper. They provide tables with error estimates of drift in x and y directions for different categories of ice concentration and ice drift speed for all three data sets. We have added a more detailed description of how we retrieve the errors.

p6, Figure 1: make figure larger (full page), arrows are hard to see.

Done.

p7, Figure 2: make larger

Done.

p8, Figure 3: make larger

Done.

p9, l8/9: Do you mean Table 3?

Yes, indeed. Thank you. Corrected.

p9, l18: this is definitely related with the EGC location, which floes along the shelf edge (haven't checked but which probably is at 6W at that latitude then). See e.g. papers by de Steur et al.

We have checked this, and included another reference by Steur et al..

p10, l5: SIC is not shown in Figs 2 & 3. What do you mean?

Thank you for pointing this out. This was indeed not entirely clear from the text. We have now included a figure also showing the ice concentration at the gate for the entire time series to clarify what is meant here.

p10, Table 3: Explain what % MYI means (maybe better in the text). Is a grid cell MYI if there was any MYI detected within the month or does it have to be >50%? What are the uncertainties of this MYI % values? Also, how does the MYI product define the MYI ice type? Is >50% MYI fraction within a grid cell considered MYI or 100% etc.?

The OSISAF ice type product only provides binary values for ice type, e.g. FYI or MYI. The percentage gives the fraction of grid cells that indicate MYI along the gate. We have added a paragraph in section 2.3 to shortly explain how the product is derived and what the uncertainties are.

p11, l4: here you are reporting on per grid cell values. That should be mentioned. Because without the grid size of 25km these values are quite hard to set into relation for the common reader.

Thank you for pointing this out. We have added: „The maximum values have to be considered in relation to the 25 km grid resolution and are likely different on smaller scales".

p11, l10: see comment for Table 3. Explain better what "majority fraction MYI" means.

We added a paragraph in section 2.3 for better explanation.

p11, l19. What are the correlation coefficients? Actually, the exports correspond less from what I would have expected from Fig. 6a. Please explain in more detail why, e.g., NSIDC in 11/12 goes down while the other two go up.

Figure 6a only shows the export along the gate and reveals a strong correlation between the products. We have included monthly export estimates using the different drift estimates. The correlation coefficients between the monthly estimates of the different products are > 0.9 and indicate similar variability. However, it seems that there are seasonal biases, especially considering NSIDC in 2011/2012.

p12, l6: I am not sure I agree with that conclusion. If NSIDC goes down in 11/12 while the other two go up, the variability is quite different, or? Similar for 13/14 to 14/15, where OSISAF & NSIDC show strong increase and IFREMER is more neutral.

As mentioned above, this is mostly due to seasonal differences. Considering the monthly export rates, the correlation coefficients between the products are > 0.9.

p12, l7: It is understood that you do not make a ice drift dataset validation study. However, your export estimates do not agree within their uncertainty estimates. Which means either your uncertainty estimates are wrong or you need to justify why you trust one dataset more than another. To me also the inter-annual variability in Fig. 6b is quite different for the three products. Some explanation for that should be added.

The estimated drift uncertainties do not contain potential biases. In Sumata et al. (2014, 2015), it is shown that these drift products are subject of systematic errors. The reason why we use OSISAF here as a reference is that it shows the best performance in the Fram Strait among the products used in this study. On the other hand, it is shown that the three products coincide quite well regarding the monthly variability (correlation between the products > 0.9). Therefore, the main results of our study are independent of the used drift product.

p12, l13: in

Corrected.

p13, Figure 7: shades of gray are hard to discern; caption: remove (b) at the end.

Fixed. We have chosen different line colors in the plot to increase readability.

p14, l1: Not "on the other hand". This argument also supports moving the gate north.

Yes, this word choice might be confusing. Corrected by using “in addition” instead.

p14, l19/20: this is supported by the overlap of STD of this study with previous studies for most months.

Yes, exactly. Exceptions are March and April. But in addition, also the other factors (2-5) will probably play a role here.

p14, l22/23: are there estimates of ice thickness gradient between 80 and 82◦N? What gradient does CS2 show? Can you estimate the thickness gradient to support this argument?

This definitely deserves more research. However, using CryoSat-2 thickness estimates for this purpose is not straight forward. South of 82°N, thickness estimates become more and more uncertain, due to the lower CryoSat-2 orbit coverage and higher ice drift.

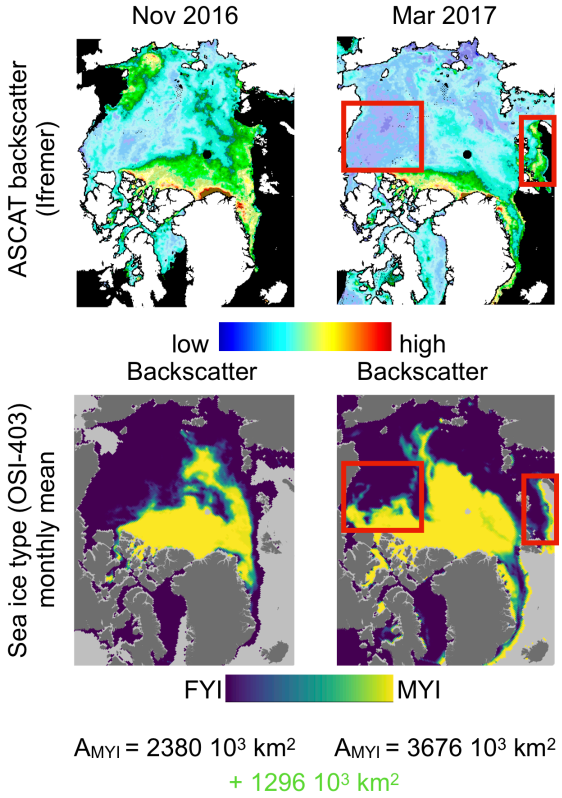

Figure R2: Monthly ASCAT backscatter maps from Ifremer and monthly averaged sea ice type from OSISAF for November 2016 and March 2017. MYI area shows a gain of more than 50% from November to March 2017, which seems unlikely.

p15, l15: Have also a look at Kwok et al. (2013), which analyses ice area export in connection to different atmospheric indices (AO, DA).

Thanks for pointing on this study. We have cited it with regard to the AO and its linkage to ice export.

p17, l5: what happened to the 7th year 16/17?

This winter season 2016/2017 has been excluded, because some obviously erroneous MYI classification has been observed, see Figure R2. We have been in contact with OSISAF therefore, and they are aware of this behavior. It might be linked to the unusual warm winter in 2016/2017 and needs further investigation. We have added an explanation in the text.

p17, l6: “Scattergram"

We have removed this sentence to reflect changes to the figure.

p17 l10: See my mayor comment at the top. I don’t think this is correct. dV_MYI/dt should almost never be positive.

As stated above, we think that thermodynamic growth can play a role also for MYI, certainly if it is undeformed second-year ice with a decreased thickness after the summer melt. But surely, the uncertainty in the ice type discrimination plays an important role, too. Therefore, we reformulated this paragraph.

p17, l15. hm, that is maybe correct. The word "variations" is not very well defined, maybe better standard deviation? However, only 29% of the variance of dV_MYI/dt is explained by Q_MYI.

We have already calculated R^2. Therefore, it gives us the percentage variation in dV_MYI/dt explained by Q_Ex_MYI.

p17, 26: yes, there are some similarities in their variability but actually their variability differs quite significantly and they do not agree within their uncertainty estimates. I find this conclusion too positive or at least need some explanation of the problems. Having results that do not agree within their uncertainty but not to mention that I do not find acceptable. Actually, I would prefer that you guide the reader which estimate they should use or you have to increase the uncertainty estimates.

As mentioned above, the uncertainty estimates do not include a bias correction and the main difference between the products is due to systematic differences. However, the correlation between the monthly volume export derived with the 3 different drift products is > 0.9. We have included the correlation coefficients between the products in the paper now. In the beginning of section 3, we refer to Sumata et al. (2014), which shows that OSISAF ice drift reveals the best performance in the Fram Strait.

p18, l7: "explained" to what degree? Give numbers.

We now state the correlation coefficients.

p18, l9: How is "variability" defined if quantitative numbers are given here?

We acknowledge that using „variability" in this context is a bit confusing. It should be Arctic MYI volume change, since we consider dV/dt.

p18, l11-13: I do not agree with this point. See explanations above.

As mentioned above, we agree that a potential bias due to erroneous ice type classification could affect dV_MYI/dt. We have removed this conclusion from the list.

p19,l17: please provide information how and where to obtain this user guide.

We have added a link that directly points on the pdf. Thank you for pointing on this.

FIxed.

P3L9: “Table 1” -> “Table 3”

Fixed.

Satellite-derived ~~sea-ice~~ sea ice export and its impact on Arctic ice mass balance

Robert Ricker[1,2], Fanny Girard-Ardhuin[2], Thomas Krumpen[1], and Camille Lique[2]

[1]Alfred Wegener Institute, Helmholtz Centre for Polar and Marine Research, Bremerhaven, Bussestrasse 24, 27570 Bremerhaven, Germany

[2]Univ. Brest, CNRS, IRD, Ifremer, Laboratoire d'Oceanographie Physique et Spatiale (LOPS), IUEM, 29280, Brest, France

Correspondence to: Robert Ricker (Robert.Ricker@awi.de)

Abstract. ~~Ice volume export drives variations of Arctic ice mass balance. It also represents a significant~~ Sea ice volume export through the Fram Strait represents an important fresh water input to the North Atlantic, which could in turn modulate the intensity of the thermohaline circulation. It also contributes significantly to variations of Arctic ice mass balance. We present the first estimates of winter sea ice volume export through the Fram Strait using CryoSat-2 sea ice thickness retrievals and three different drift products for the years 2010 to 2017. The ~~export rates vary~~ monthly export varies between -21 and -540 km^3~~/month~~. We find that ice drift variability is the main driver of annual and interannual ice volume export variability, and that the interannual variations of the ice drift are driven by large scale variability of the atmospheric circulation captured by the Arctic Oscillation and North Atlantic Oscillation indices. On shorter timescale, however, the seasonal cycle is also driven by the mean thickness of exported sea ice, typically peaking in March. Considering Arctic winter multiyear ice volume changes, 54 % of ~~the~~ their variability can be explained by the variations of ice volume export through the Fram Strait.

1 Introduction

Variability of the Arctic sea ice export contributes significantly to the variations of surface salinity in the subpolar gyre, and in particular in the regions where deep convection occurs, such as the Labrador and Greenland Seas. Fram Strait ice export represents approximately 25% of the total fresh water export to the North Atlantic (Lique et al., 2009). By the impact on convective overturning of water masses in the North Atlantic, changes in the export rates could affect the global ocean thermohaline circulation (Dickson et al., 1988). A recent study by Ionita et al. (2016) reports that persistent atmospheric blocking in winter leads to increased sea ice export through the Fram Strait, causing abrupt shifts in the Atlantic meridional overturning circulation variability. In turn, this might also affect the climate over Europe.

~~Variability of the Arctic sea-ice mass balance is determined by sea-ice production and melt on the one hand, and sea ice export on the other hand. Arctic sea ice~~ Arctic sea ice volume and related interannual variations have been investigated for the winter season (October-April) in various recent studies, using satellite altimetry (Tilling et al., 2015; Kwok and Cunningham, 2015; Ricker et al., 2017a). ~~The Fram Strait represents the main Arctic gate for sea ice export. While iceexport rates during summer are relatively low (Krumpen et al., 2016), winter ice export plays an important role for the multiyear~~ While first-year sea ice (FYI) volume reveals a distinct seasonal cycle between October and April due to thermodynamic growth and new forming ice, multiyear sea ice (MYI) mass balance in the Arctic (Kwok et al., 1999). volume shows only small changes within this period (Ricker et al., 2017a).

MYI is defined as sea ice that survived at least one summer melt periodand significantly contributes to the exported sea ice (Kwok et al., 1999). Its greater age implies that it went through a longer period of thermodynamic ice growth and additional thickening due to deformation. Therefore, MYI can reach several meters of thickness, making it resistant against storms and melting . Hence, melting and storms. Parkinson and Comiso (2013) have shown that storms like in August 2012 can cause a break up of the weakened ice surface, leading to a reduction of ice area. MYI attenuates potential loss of ice coverage due to external forcing, while the thinner first-year ice (FYI) FYI is much more sensitive to storms and temperature fluctuations (Holland et al., 2006). As a consequence, summer ice concentration strongly correlates with MYI coverage, highlighting its climate relevance (Comiso, 1990; Thomas and Rothrock, 1993). Multiple studies Maslanik et al. (2011) have shown that Arctic MYI fraction has been shrinking during the last decades, from about 75% in the mid 1980s to 45% in 2011 (Maslanik et al., 2011). 2011. Indeed, anomalously large summer melt reduces the MYI volume and prevents its replenishment by aging FYI (Stroeve et al., 2014; Kwok, 2007).

In The variability of the Arctic sea ice mass balance is determined by sea ice production and melt on the one hand, and sea ice export on the other hand. The Fram Strait represents the main Arctic gate for sea ice export. While ice export rates during summer are relatively low (Krumpen et al., 2016), winter ice export plays an important role for the MYI mass balance in the Arctic (Kwok et al., 1999). Therefore, in order to improve our understanding of these processes that are linked to the variability of Arctic MYI mass balance, monitoring winter sea ice volume export through the Fram Strait is crucial. Only satellite measurements have the capability to continuously monitor pan-arctic changes in ice concentration, thickness and drift, the parameters required for calculating ice volume flux. Spreen et al. (2009) estimated Fram Strait sea ice volume export between 2003 and 2008. They used ICESat laser altimeter observations to derive sea ice thickness and AMSR-E 89 GHz passive microwave data to retrieve sea ice concentration and drift. A comparison with previous estimates that were based on a parametrization of ice thickness (Vinje et al., 1998; Kwok and Rothrock, 1999) and drift (Vinje et al., 1998) did not indicate a significant change of the total amount of Fram Strait sea ice export between the 1990s and 2008. However, one needs to keep in mind that ICESat measurements were restricted to two periods per winter season, and thusOctober/November and February/March. Thus, investigations on the seasonal cycle of ice volume export were limited. The European Space Agency (ESA) satellite CryoSat-2 (CS2) was launched in 2010 and partly overcomes these limitations (Wingham et al., 2006) as monthly Arctic wide CS2 sea-ice sea ice thickness estimates are derived between October and April (Tilling et al., 2016; Ricker et al., 2014). This allows to produce unrivaled monthly estimates of ice volume export using satellite data and contributes to overarching objectives, such as the quantification of fresh water input from the Arctic to the subpolar North Atlantic, affecting the Atlantic meridional overturning circulation.

In this study, we pursue four main objectives. First, we use the Alfred Wegener Institute (AWI) CS2 ice thickness data set (Ricker et al., 2014) to estimate for the first time winter sea ice export through Fram Strait over 7 years between 2010 and 2017 (October-April) and compare our estimates with previous studies. We use three different low-resolution ice drift products in order to access assess the impact of the chosen drift data set. Second, we aim to examine the temporal variability of volume

Table 1. Ice drift products used for this study.

Name	Product	Input data	Temporal resolution	Spatial resolution	Period
OSISAF	OSI-405 (merged)	SSMIS (91 GHz, DMSP F17), ASCAT (Metop-B), AMSR-2 (18.7 and 36.5 GHz)	48 h	62.5 km	2009 - 2017
IFREMER	CERSAT (merged)	QuikSCAT, ASCAT (MetOp-A , Metop-B), SSM/I (85 GHz), SSMIS (91 GHz)	1 month	62.5 km	1991 - 2017
NSIDC	Polar Pathfinder v3.0	AMSR-E (89 GHz), SSM/I (85 GHz), SMMR (37 GHz), AVHRR, buoy position, NCEP/NCAR wind data	1 month	25 km	1978 - ~~2015~~ 2017

export and its links with variability in sea ice drift, thickness and concentration. We then relate the interannual variability of ice volume export through Fram Strait to the variability of the atmospheric circulation captured by the Arctic Oscillation and North Atlantic Oscillation indices. Our fourth objective is to quantify the impact of winter ice volume export on Arctic sea ice mass balance, which will be achieved by considering Arctic net monthly ice volume changes.

The paper is organized as follows. Section 2 describes the CS2 ice thickness product, the used ice drift data and ancillary data sets. In section 3, we first examine spatial and temporal variability of sea ice thickness, drift and ice concentration at the Fram Strait gate and present estimates of the ice volume flux and Fram Strait export. The seasonal and interannual variability of ice volume export and its impact on Arctic ice mass balance are discussed in section 4. Conclusions are drawn in section 5.

2 Data and Methods

In this section, we describe data products used in this study, as well as methods to retrieve ice volume fluxes through the Fram Strait. Table 1 summarizes the specifications of the ice drift products. In addition to ~~drift,~~ ice drift, also ice thickness and concentration data are required to estimate ice volume fluxes.

2.1 Sea Ice drift

2.1.1 OSI SAF

We use the low resolution sea ice drift data set from the Ocean and Sea Ice Satellite Application Facility (OSI SAF), specifically the OSI-405 multi sensor product. Various sensors and channels are processed in order to produce the merged product used here: SSMIS (91 GHz H&V polarization) on board DMSP platform F17, ASCAT (C-band backscatter) on board platform Metop-A, and AMSR-2 on board JAXA platform GCOM-W. Ice drift is estimated by an advanced cross-correlation method

(Continuous MCCMaximum cross-correlation (MCC)) on pairs of satellite images (Lavergne et al., 2010). The merged product considers the different single sensor data and their quality statistics in order to compensate for data gaps in the single sensor products. We use this multi sensor data set, since we require a sufficient data coverage in the Fram Strait area, which is not given by the single sensor products. Displacements and geographic coordinates of the start and end point of the displacements for 48 h time spans are provided on a 62.5 km x 62.5 km polar stereographic grid. In the following we refer to this product as *OSISAF*.

2.1.2 Ifremer

From Ifremer/CERSAT, we use the merged product, which is obtained from combining Advanced Scatterometer (ASCAT) data and special sensor microwave/imager (SSM/I) brightness temperature measurements. It is provided for different time spans, including monthly lags, which is suitable for our study. The algorithm to deduce ice drift from scatterometer data and the merging with radiometer data is described in Ezraty et al. (2007) and Girard-Ardhuin and Ezraty (2012). Geographic coordinates of the start and end point of the displacements are provided on a 62.5 km x 62.5 km polar stereographic grid. In the following we refer to this product as *IFREMER*.

2.1.3 NSIDC

Finally, we also use the Polar Pathfinder Sea Ice Motion Vectors (version 23), distributed by the National Snow and Ice Data Center (NSIDC). It provides a year-round ice drift data set. As for OSISAF and IFREMER, ice drift is obtained from multiple satellite sensors including radiometers and scatterometers (Table 1) complemented by buoy observations from the International Arctic Buoy Program (IABP). During summer, NCEP/NCAR winds speeds are used to estimate ice drift when satellite data are not available. Though we do not make use of the summer ice drift data, we choose to include this data set, since it is widely used in other studies (e.g. Krumpen et al. (2016) and Spreen et al. (2011)). Monthly Displacements in x and y direction are provided on an EASE 2 25 km x 25 km polar stereographic grid. In the following we refer to this product as *NSIDC*. In contrast to OSISAF and IFREMER, NSIDC is only available until February 2017, which means that we do not consider winter season 2016/2017 for NSIDC.

2.2 AWI CS2 sea ice thickness

We use the AWI CS2 product (processor version 1.2). Processing is based on CS2 orbit data files provided by ESA. Radar waveforms are processed according to Hendricks et al. (2016) and Ricker et al. (2014), using a 50% threshold-first-maximum retracker to obtain ellipsoidal surface elevations (Ricker et al., 2014; Helm et al., 2014). Radar waveforms from surfaces that contain openings in the ice pack appear as specular echoes and can be separated from diffuse echoes that contain reflections from sea ice only. Based on this surface type classification, open water elevations are identified and used to derive the instantaneous sea-surface height anomaly by interpolation. To retrieve sea ice freeboard, the sea-surface height anomaly is subtracted from the ice surface elevations.

Freeboard is converted into sea ice thickness by assuming hydrostatic equilibrium (Laxon et al., 2003). For the conversion, we use ice densities of 916.7 kg/m^3 and 882.0 kg/m^3 for FYI and MYI respectively (Alexandrov et al., 2010), and 1024 kg/m^3 for the sea water density. Snow depth and density are deduced from the Warren snow climatology (W99) (Warren et al., 1999). The climatology is modified by reducing the snow depth by 50 % over FYI to take into account the recent change towards a seasonal Arctic ice cover. FYI and MYI are identified with the daily OSI SAF sea ice type product (Eastwood, 2012). In order to obtain a sufficient spatial coverage, acquired thickness data are averaged monthly on an 25 km EASE 2 grid.

The CS2 observational uncertainties of sea ice thickness contain contributions that are associated with speckle noise, sea-surface height estimation, snow depth, and densities of ice and snow (Ricker et al., 2014). They can easily reach values of > 1 m for single measurements, but will be reduced to the range of centimeters by spatial averaging. Note that during the melting period from May to September, the presence of melt ponds prevents the retrieval of sea ice thickness observations.

2.3 OSI SAF Ice concentration and type

We use the ~~OSI SAF sea-ice concentration and type products (OSI-401-b) and~~ sea ice concentration (~~OSI-403-b), respectively (Eastwood, 2012). Ice~~ OSI-401) and sea ice type product (OSI-403) of the European Organisation for the Exploitation of Meteorological Satellites (EUMETSAT) Ocean and Sea Ice Satellite Application Facility (OSI SAF). Ice concentration is computed from radiometer data, using a combination of state-of-the-art algorithms (Tonboe et al., 2017). Ice type is derived from passive microwave and active microwave scatterometer data combined in a Bayesian approach (Aaboe et al., 2016). Ice concentration is needed for the ice volume computation for each 25 km grid cell and ice type is used to classify grid cells as FYI or MYI. The products are updated daily and the data are provided on a 10 km polar stereographic grid. To be consistent with the CS2 product, monthly means are projected onto the EASE2 25 km grid. ~~Grid~~ Ice type grid cells originally flagged as *ambiguous* are replaced by an inverse-distance interpolation to obtain FYI or MYI flags for all ice-covered grid cells. Errors can occur due to new forming openings within the MYI zone that are not captured and therefore classified as MYI. Especially in the Fram Strait, where floes can break up into many smaller pieces, this might lead to significant errors in MYI fraction. Moreover, we have observed erroneous MYI classification in the Arctic Basin during winter 2016/2017. The reason is not yet clear, but could to be a result of external factors such as exceptional warm winter temperatures. Therefore, FYI/MYI separation for 2016/2017 should be considered with caution (S. Aaboe, personal communication, 2017).

2.4 Retrieving ice volume flux and export rates through Fram Strait

The first step is to project the ice drift and thickness data onto a common grid. The EASE 2 grid is based on an equal area projection, and therefore, it is reasonable to use it for ~~sea-ice~~ sea ice volume estimations (Ricker et al., 2017a). Hence, we define the 25 km EASE 2 grid provided in the AWI CS2 ice thickness product as our standard grid and interpolate the displacement data onto this grid. Since the NSIDC displacement data are already projected on an EASE grid, we only interpolate the displacements in x and y direction onto the 25 km grid. In contrast, the IFREMER and OSISAF grids are based on a polar stereographic projection. Here, we use the geographic coordinates of the start and end point of the displacement and project them onto the EASE 2 grid separately. Afterwards, displacements in x and y direction of the EASE 2 grid are calculated.

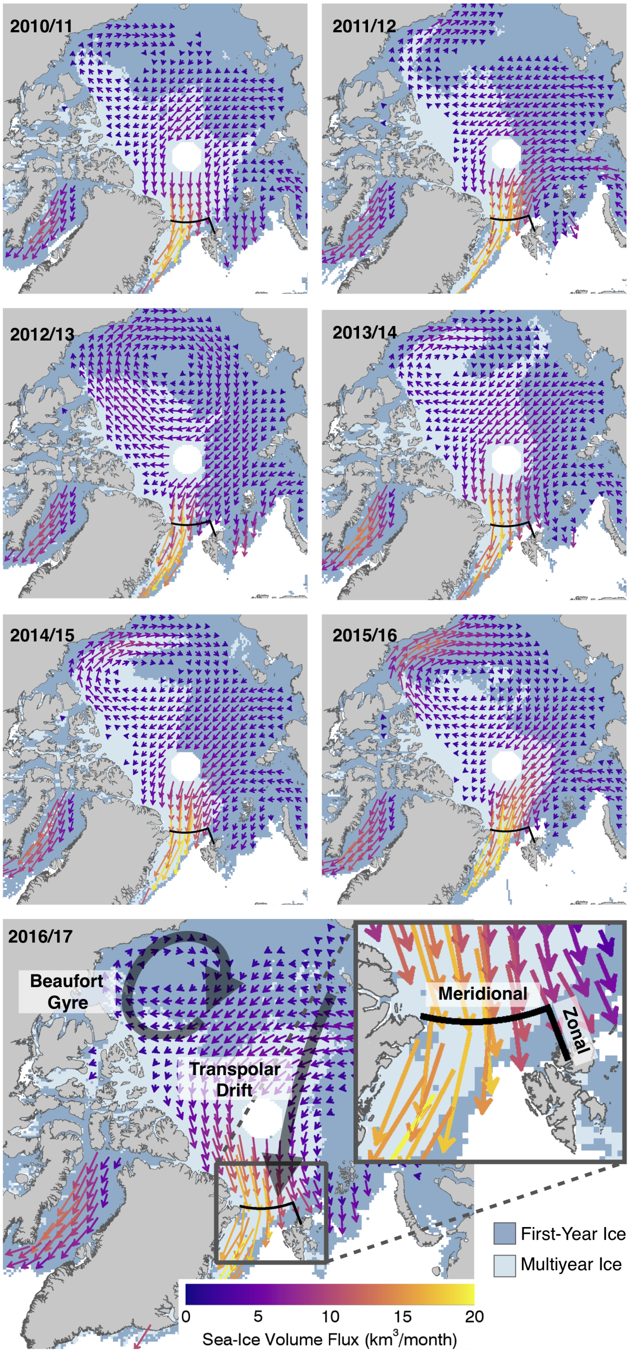

Figure 1. Means of Arctic ~~sea-ice~~ sea ice volume fluxes for 2010/2011 - 2016/2017 between October and April. The enlarged box shows the location of the Fram Strait gate at 82°N, which is used for the calculation of the export rates, separated into meridional and zonal gates.

Since the Ifremer product is IFREMER and NSIDC products are provided as monthly means, the daily updated OSISAF 48 h displacements need to be averaged monthly summed up to monthly retrievals. Here, we calculate the displacements in x and y direction on the EASE 2 grid for each day and average them sum them up over one month.

Monthly ice volume flux $Q_{x,y}$ in x and y direction is obtained by:

$$Q_{xy} = lHCD_{xy}, \tag{1}$$

where l = 25 km is the size of the grid cells, H is the CS2 sea ice thickness, C is the ice concentration obtained from the OSISAF product, and D_{xy} represents the ice drift in x and y direction respectively.

In order to compute ice volume export through Fram Strait, we follow the methodology of Krumpen et al. (2016) and define a gate that is a composite of a meridional and a zonal gate (Figure 1). The meridional gate is located along 82°N between 12°W and 20°E. The zonal part is located along 20°E between 80.5°N and 82°N. We have chosen this gate location to reduce errors and biases in low resolution ice drift data that become larger with increasing ice velocities, typically found south of 82°N (Sumata et al., 2014, 2015). Moreover, uncertainty of CS2 ice thickness increases at lower latitudes, especially near Fram Strait due to sparse orbit coverage (Ricker et al., 2014).

Meridional (Q_v) and zonal (Q_u) components components Q_v of the ice volume flux through the defined gate are calculated as follows:

$$Q_v = l/\cos(\lambda)_{uv} HC(D_x \sin(\lambda) - D_y \cos(\lambda))_v$$

$$Q_{uv} = l/\cos(\lambda)_{uv} HC(D_x \cos\sin(\lambda) - D_y \sin\cos(\lambda)),. \tag{2}$$

The zonal components Q_u of the ice volume flux are computed accordingly:

$$Q_u = l_{uv} HCD_u$$

$$Q_u = l_{uv} HC(D_x \cos(\lambda) + D_y \sin(\lambda)), \tag{3}$$

where λ is the longitude of the respective grid cell . Uncertainties of Q and l_{uv} the length of the grid cell as a function of λ:

$$l_{uv} = l/\cos(\lambda) \tag{4}$$

Uncertainties of Q_v are estimated by:

$$\sigma_{QQ_v} = l/\cos(\lambda)\sqrt{(HC\sigma_D)^2 + (DC\sigma_H)^2 + (HD\sigma_C)^2}_{uv}\sqrt{(HC\sigma_D)^2 + (D_vC\sigma_H)^2 + (HD_v\sigma_C)^2}. \tag{5}$$

Meridional uncertainties σ_{Q_u} are calculated accordingly. Consistent with Laxon et al. (2013) and Ricker et al. (2017a), we set the ice-concentration uncertainty $\sigma_{\mathrm{c_i}}$ = 5%. Nevertheless, we acknowledge that the uncertainty may vary depending on the actual ice concentration (Ivanova et al., 2014). Sea ice thickness uncertainty σ_H is provided in the AWI CS2 ice thickness product (Ricker et al., 2014). Ice drift uncertainty σ_D is estimated using the empirical error functions for monthly mean Arctic sea-ice sea ice drift given in Sumata et al. (2015). This study , which utilizes drift estimates from high-resolution SAR data as a reference. Drift uncertainties of low resolution monthly mean products in :

$$\sigma_D = \sqrt{\epsilon_x^2 + \epsilon_y^2}, \tag{6}$$

with the drift error functions $\epsilon_{x,y}$ in x and y direction of the grid used in Sumata et al. (2015):

$$\epsilon_{x,y} = \sqrt{\sigma_{x,y}^2 + \delta_{x,y}^2}, \tag{7}$$

where $\sigma_{x,y}$ are standard errors in x and y directions are provided for different drift speeds and ice concentrations. These uncertainties are then combined with the uncertainty given in Sumata et al. (2015) for different categories of drift speed and ice concentration for each of the three drift products. Here, we use standard errors for the highest drift speed (> 4.3 km/d). $\delta_{x,y}$ represents the error of the reference ice drift drift data set, provided in Sumata et al. (2015). The deduced drift uncertainties for the low resolution drift products are in the range of 1.0 km/d, which is comparable to uncertainties estimated in previous studies (Spreen et al., 2009). These estimates do not include systematic errors. A comparison of different drift products in Sumata et al. (2014) shows significant systematic differences between the different drift products, especially for high drift speeds. Since we aim to investigate variabilities in ice volume export, we do not consider potential biases in this study.

We obtain the total ice volume flux through the Fram Strait (Q_{Ex}) by adding up the meridional zonal grid cell fluxes Q_v and Q_u along the gate:

$$Q_{\mathrm{Ex}} = \sum Q_u + \sum Q_v. \tag{8}$$

Note that following the axes conventions, ice volume export Q_{Ex} has a negative algebraic sign, corresponding to a sea ice loss from the Arctic Basin.

3 Results

In this section, we first examine sea ice drift, thickness and concentration at the Fram Strait gate. Throughout the study, we use the OSISAF drift as the reference product, because it shows the best performance among the used products in the Fram Strait (Sumata et al., 2014). Second, we present estimates of the ice volume flux in the Arctic and the calculated export through Fram Strait. Third, we examine the choice of the drift product, computing ice volume export using also IFREMER and NSIDC ice drift estimates. Throughout the paper, we refer to the winter period from October to April (OA). However, seasonal export estimates are calculated adding together monthly export from November to April (NA), since we have no ice thickness estimates for October 2010.

3.1 Sea ice drift, thickness and concentration at the gate

We consider all input parameters for Eq. (1), sea ice thickness (H), sea ice drift (D), and ice concentration (C). Figure 2 shows the spatiotemporal distribution of CS2 ice thickness along the meridional and zonal gates through each winter season,

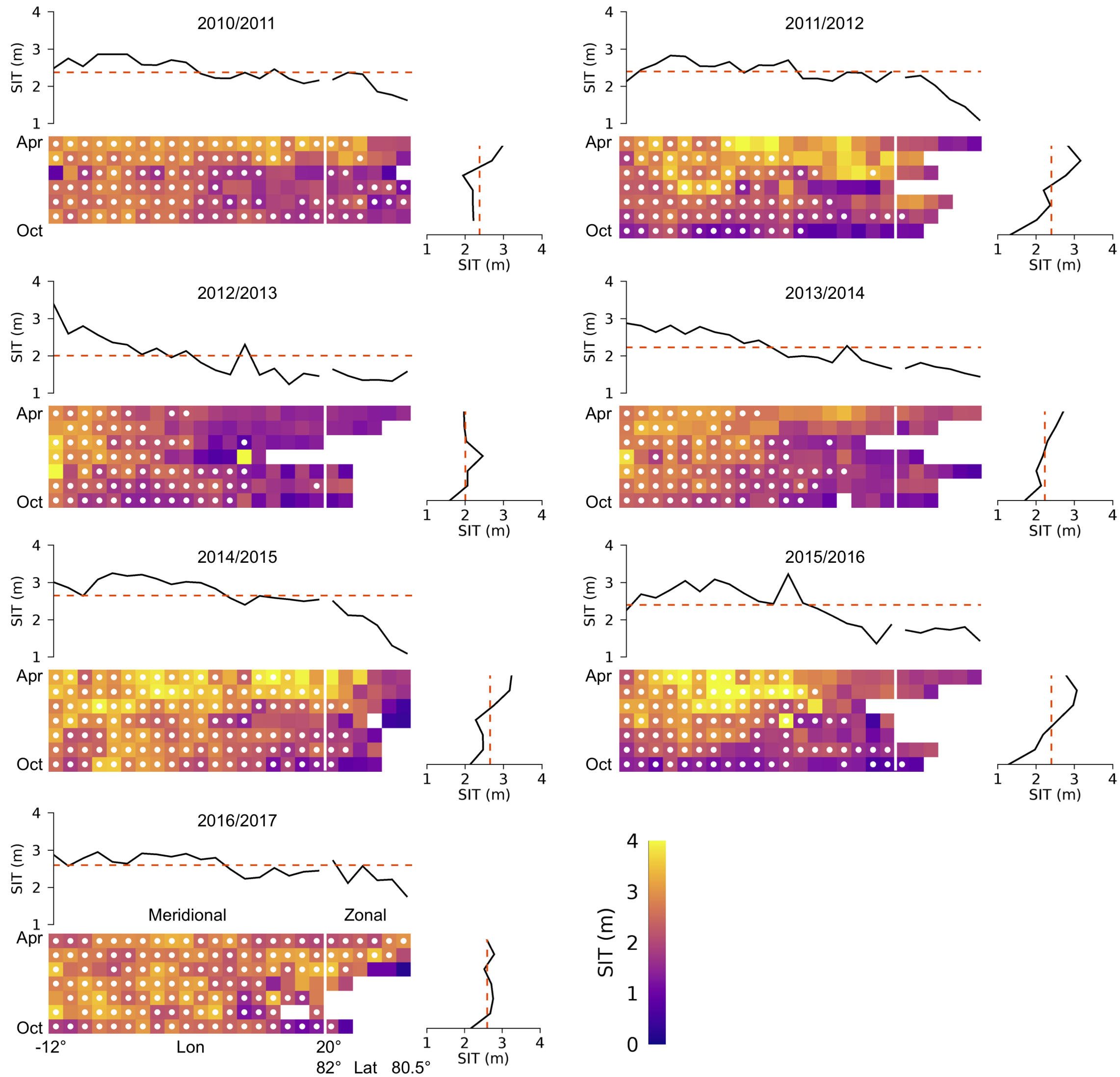

Figure 2. Spatiotemporal variability of sea ice thickness (SIT) at the Fram Strait gate from October to April between 2010 and 2017. Upper sub-panels show the temporal averaged SIT. Right sub-panels show the average over the gate SIT for each month within the October-April period. The white dots represent grid cells that contain multiyear ice.

separated into FYI and MYI. Ice thickness along the gate is variable and ranges from 0 to 5 m. The mean gate thickness reveals a consistent gradient from thinner ice in October to thicker ice in April in all years, although the gradient can be small for some years (e.g. 2016/2017). Averaging over each OA period reveals the spatial thickness distribution along the meridional and zonal gates. In 2012/2013 and ~~2012/~~2013/2014, we find a significant positive thickness gradient towards the coast of Greenland, while in other years, this is less pronounced. At the zonal gate, ice thickness decreases towards Svalbard. ~~As indicated in Table 1,~~

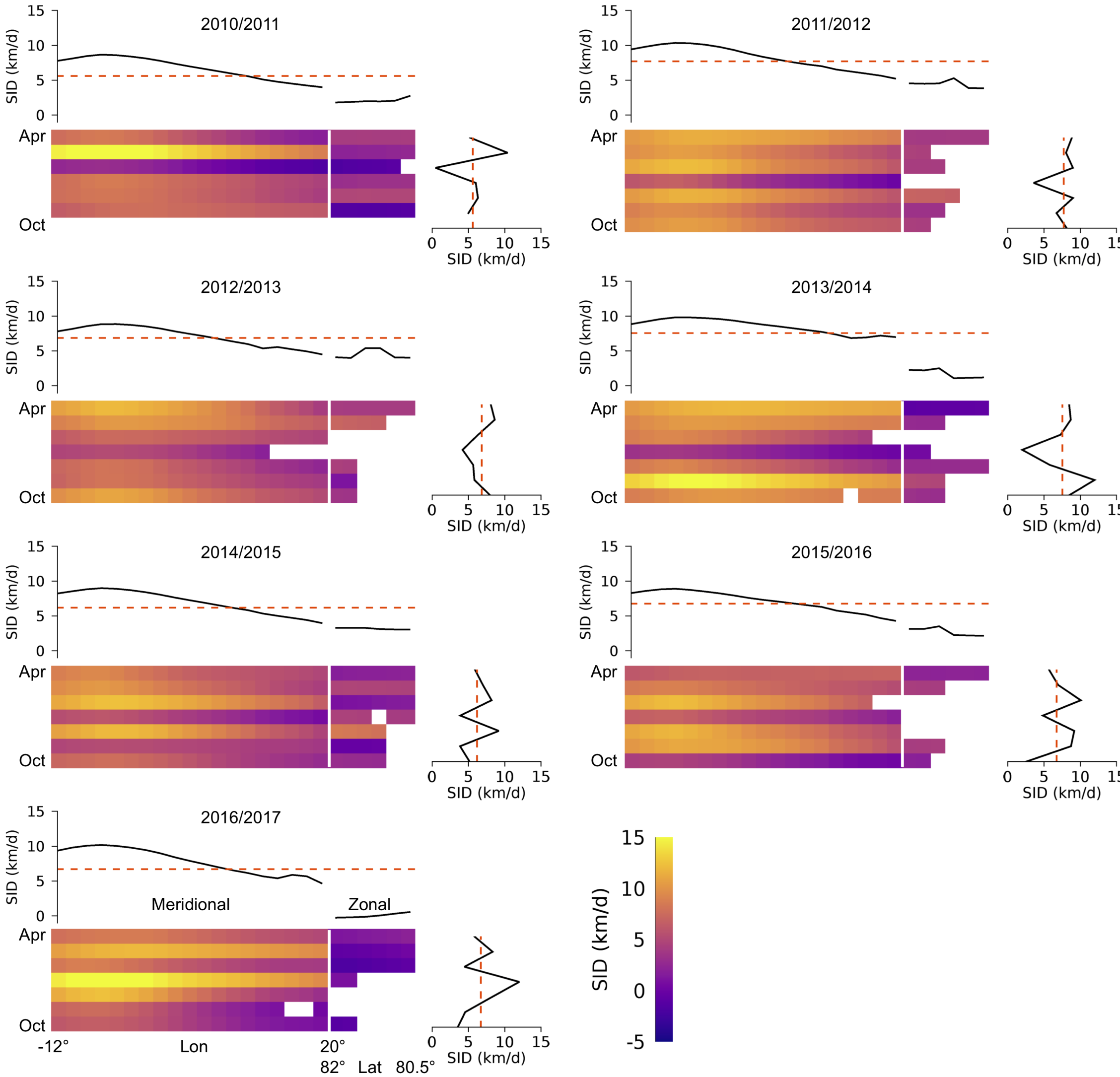

Figure 3. Spatiotemporal variability of OSISAF sea ice drift (SID) at the Fram Strait gate from October to April between 2010 and 2017. Upper sub-panels show the temporal average SID. Right sub-panels show the average over the gate SID for each month within the October-April period.

~~during~~ During winter seasons 2011/2012, 2012/2013 and 2013/2014, ~~MYI fraction~~ fraction of grid cells that contain MYI is lower compared to other years. In 2012/2013 and 2013/2014, the lack of MYI in the eastern part of the gate is replenished by FYI that is thinner than 1.5 m. In seasons 2010/2011 and 2016/2017, MYI fraction at the zonal gate is larger than in other years. In 2011/2012, from February to March, the indicated FYI is rather thick (> 2 m), similar to the indicated MYI towards the coast of Greenland.

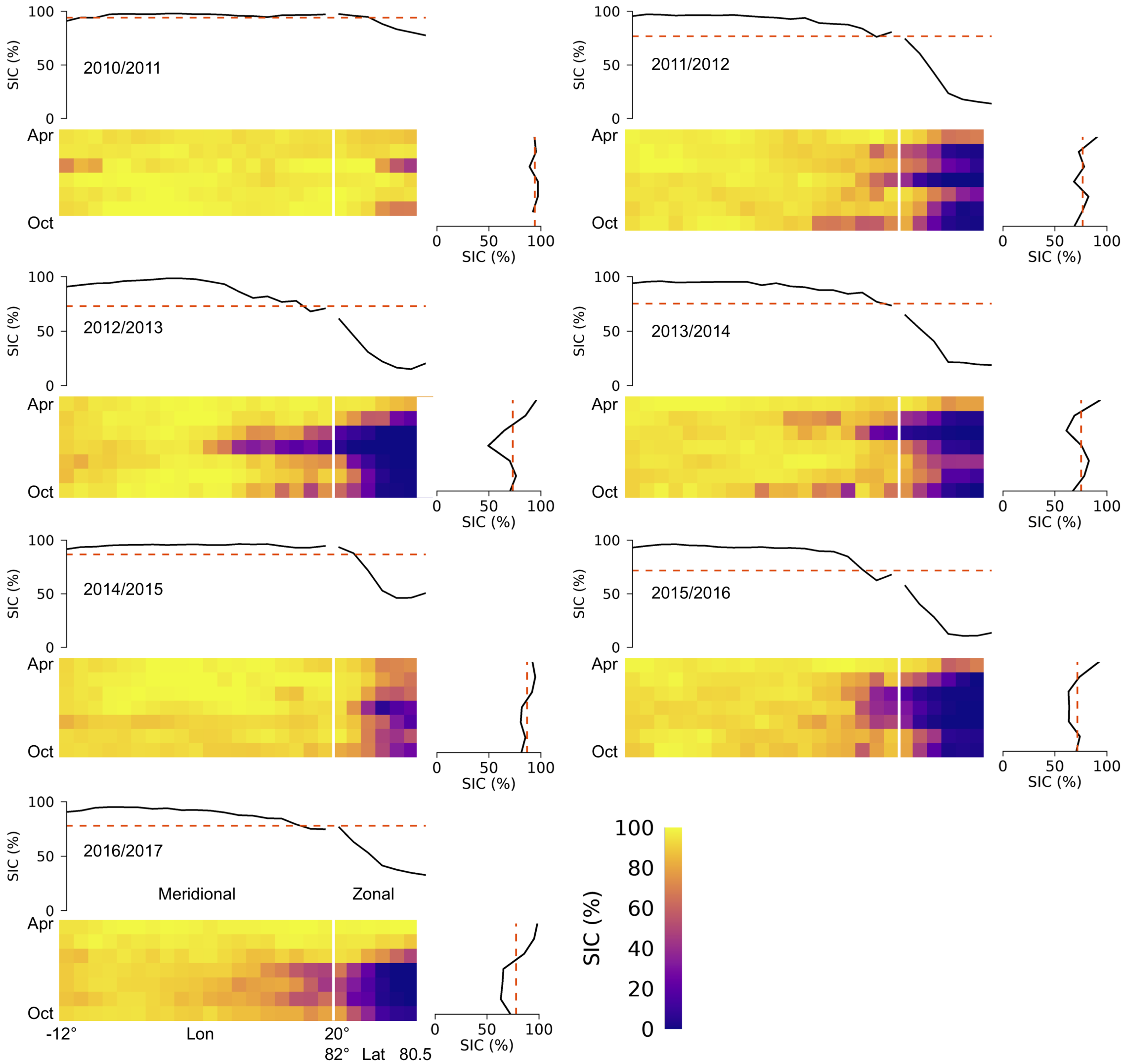

Figure 4. Spatiotemporal variability of OSISAF sea ice ~~drift, ice thickness, and ice~~ concentration ~~averaged over~~ (SIC) at the ~~entire~~ Fram Strait gate ~~, between~~ from October ~~and~~ to April ~~for winter seasons~~ between 2010 ~~/2011 to 2016/~~and 2017. ~~The right box shows~~ Upper sub-panels show the ~~corresponding histograms with~~ temporal average SIC. Right sub-panels show the ~~overall means and relative standard deviations (RSD)~~average over the gate SIC for each month within the October-April period.

Figure 3 shows the spatiotemporal distribution of the OSISAF ice drift along the meridional and zonal gates through each winter season. In contrast to ice thickness, the drift reveals a larger temporal variability with monthly differences of up to 10 km/d and without a distinct trend within each winter season. On the other hand, the OA period averages of the drift show a consistent spatial trend for all years, from less than 5 km/d in the east (20°E) and at the zonal gate, to a maximum of 9-10 km/d at about 6°W, followed by a decrease towards the coast of Greenland. The stationary peak at about

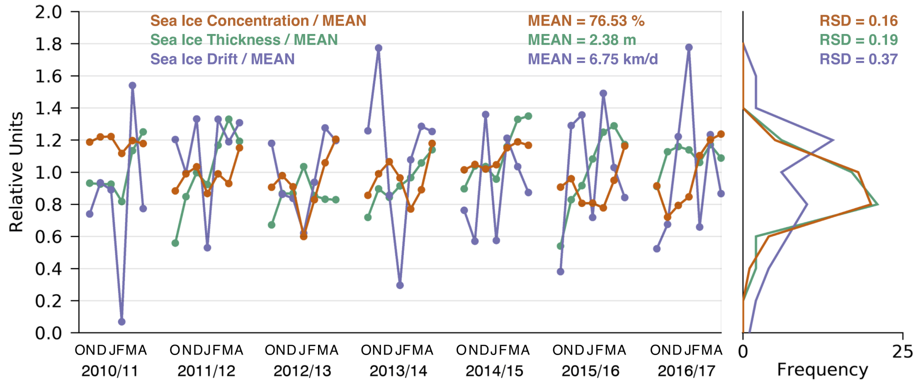

Figure 5. OSISAF sea ice drift, ice thickness, and ice concentration averaged over the entire Fram Strait gate, between October and April for winter seasons 2010/2011 to 2016/2017. Monthly values are divided by the mean of the data set for each parameter. The right box shows the corresponding histograms with the relative standard deviations (RSD).

6°W suggests a large scale forcing and could be associated with the East Greenland Current ~~(Rudels et al., 2002). We also~~ (Rudels et al., 2002; de Steur L. et al., 2009). We notice that mean drift across the zonal gate is only 35 % of the mean drift across the meridional gate. The IFREMER and NSIDC ice drift also exhibit similar patterns as OSISAF (not shown).

Figure 4 shows the spatiotemporal distribution of the ice concentration along the meridional and zonal gates through each winter season. Ice concentration at the meridional gate is persistently high and ranges between 70 % and 100 %, with few exceptions like January 2012/2013. In contrast, the zonal ice concentration shows higher variability, depending on the ice extent north of Svalbard, where the ocean remains ice free in some areas over several months.

Figure 5 illustrates ice drift, thickness, and concentration averaged over the entire gate and divided by their mean values to illustrate their variability and make it comparable. Here, ice concentration represents the fraction of ice covered area along the entire gate, including the zonal and meridional parts. ~~Ice concentration at the meridional gate typically ranges between 70 % and 100 %, while the zonal gate remains ice free in some areas over several months.~~ As indicated in ~~Figures 2and 3~~Figure 2, in contrast to ice drift, ice thickness shows a trend in most of the winter seasons. The same holds for the ice concentration as ice extent at the zonal gate north of Svalbard increases during winter ~~(Figures 2 and 3~~in most of the seasons (Figure 4). In 2010/2011, the gate was almost entirely ice covered during the OA period. The histograms refer to the drift, thickness and concentration time series over the entire 7-years period. The drift distribution reveals two modes and a larger degree of dispersion than the ice thickness and concentration distribution. In order to compare and quantify the extent of variability of the three parameters we compute their relative standard deviation (RSD), which is the ratio of the standard deviation to the mean. We find that the RSD of the ice drift (0.37) is roughly double of the RSD of ice thickness (0.19) and ice concentration (0.16).

Table 2. Monthly Arctic ~~sea-ice~~ sea ice volume export through the Fram Strait in km^3/month, computed with OSISAF ice drift.

	Oct	Nov	Dec	Jan	Feb	Mar	Apr
2010/11	–	-227	-275	-267	-21	-540	-279
2011/12	-164	-214	-354	-129	-381	-379	-487
2012/13	-203	-182	-187	-103	-163	-299	-318
2013/14	-215	-400	-231	-78	-195	-345	-452
2014/15	-200	-165	-373	-160	-425	-429	-354
2015/16	-52	-261	-275	-177	-352	-348	-310
2016/17	-129	-151	-307	-466	-201	-431	-292

Table 3. Total Arctic ~~sea-ice~~ sea ice volume export through the Fram Strait for winter seasons 2010/2011 - 2016/2017, added together over the November-April period. Volume export has been computed using three different ice drift products, using $Q_{\mathrm{Ex,OSISAF}}$ as the reference product. The last column shows the fraction of exported multiyear sea ice (% MYI).

Season	Q_{Ex} OSISAF (10^3km^3)	ΔQ_{Ex} IFREMER-OSISAF	ΔQ_{Ex} NSIDC-OSISAF	MYI (%)
2010/11	-1.61 $\pm$ 0.21	+0.22	+0.15	90
2011/12	-1.94 $\pm$ 0.22	+0.48	+0.80	68
2012/13	-1.25 $\pm$ 0.16	+0.27	+0.36	64
2013/14	-1.70 $\pm$ 0.20	+0.36	+0.55	68
2014/15	-1.91 $\pm$ 0.23	+0.48	+0.38	92
2015/16	-1.72 $\pm$ 0.19	+0.53	+0.52	81
2016/17	-1.85 $\pm$ 0.21	+0.48		94

3.2 Sea ice volume flux and export through the Fram Strait

Figure 1 shows the retrieved ice volume flux as means over the OA period for the northern hemisphere for the 7 years of the CS2 operational period (2010-2017), using OSISAF ice drift data. The two major patterns are the Beaufort Gyre and the Transpolar Drift conveying ice towards Fram Strait. There, the ice fluxes reach maximum values of 20 km^3/month or more, with a steep gradient along a north-south axis. The maximum values have to be considered in relation to the 25 km grid resolution and are likely different on smaller scales. MYI is mainly exported through the meridional part of the gate, while sea ice at the zonal part is primarily FYI. The monthly sea ice volume export through Fram Strait is shown in Table 2 and Figure ~~5~~6. During the 7-years period, the maximum monthly ice volume export of -540 km^3/month occurs in March 2011, while the minimum of -21 km^3/month is found in February 2011. Table 3 provides the total ice volume export ($Q_{\mathrm{Ex,OSISAF}}$) through the Fram Strait

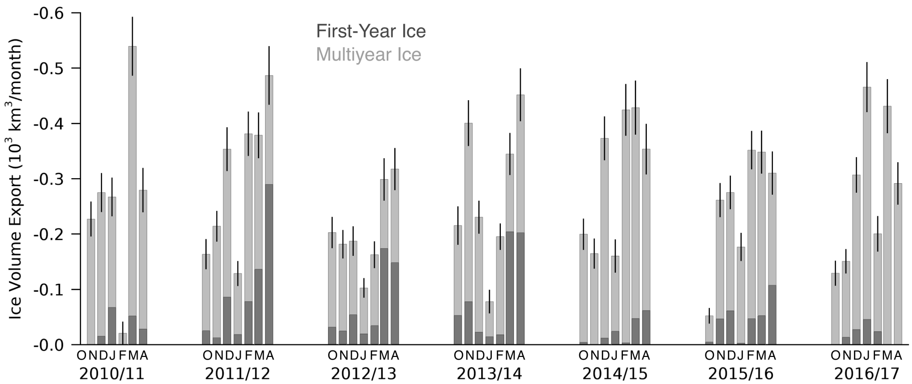

Figure 6. Monthly sea-ice sea ice volume export through Fram Strait from October to April for the period 2010/2011 - 2016/2017, using the OSISAF ice drift product. The volume export is devided divided into first- and multiyear sea ice. Uncertainties are represented by error bars. October 2010 data are missing due to unavailability of CryoSat-2 data.

gate for the NA period. We find a maximum export of -1910 ± 230 km^3 for 2011/2012 and a minimum of -1250 ± 160 km^3 in 2012/2013. The major fraction of exported sea ice is represented by MYI. However, in few months like April 2012, the fraction of exported FYI exceeds the MYI fraction. Table 3 shows the MYI fraction fraction of exported MYI averaged over the seasons. A maximum of 94 % occurs in 2016/2017 and a minimum of 64 % occurs in 2012/2013. The MYI fraction refers to grid cells which are indicated as MYI by using the ice type product.

3.3 Deriving sea ice volume export using different ice drift products

Figure 6In order to investigate the impact of the chosen drift product on the volume export estimates, we compare ice volume flux through the Fram Strait gate using three different drift products. Figure 7a shows an example for monthly ice volume flux through the Fram Strait gate and the contributions to the meridional and zonal parts of the gate, using three different the three drift products. All three retrievals exhibit consistent temporal and spatial variations along the gate, but differ in magnitude. $Q_{\mathrm{Ex,OSISAF}}$ and $Q_{\mathrm{Ex,IFREMER}}$ always exceed $Q_{\mathrm{Ex,NSIDC}}$ by about 0.2-0.3 km^3/day. Uncertainties of the ice flux through each grid cell are in the range of 0.1 km^3/day. Figure 67b shows the total monthly and seasonal ice volume export through the Fram Strait during the NA period between 2010 and 2017, computed with the three different drift products. The variations of $Q_{\mathrm{Ex,OSISAF}}$ and $Q_{\mathrm{Ex,IFREMER}}$ correlate, but differ in magnitude. Table 3 provides the corresponding annual differences between the products. Using IFREMER ice drift, the derived ice export is 200-500 km^3 lower than export derived using OSISAF ice drift, which corresponds to a mean difference of about -23 %. $Q_{\mathrm{Ex,NSIDC}}$ is the lowest among the three estimates and shows mean difference of about -26 %, relating to $Q_{\mathrm{Ex,OSISAF}}$. Also, the interannual variability changes of $Q_{\mathrm{Ex,NSIDC}}$ compared to both $Q_{\mathrm{Ex,OSISAF}}$ and $Q_{\mathrm{Ex,IFREMER}}$ is are slightly different as $Q_{\mathrm{Ex,NSIDC}}$ decreases from 2010/2011 to 2011/2012, while the other both retrievals show an increase. In 2011/2012, the monthly difference of $Q_{\mathrm{Ex,NSIDC}}$ to the other retrievals is significantly higher than in other winter seasons, but the reason for this is unclear. Nevertheless, the main

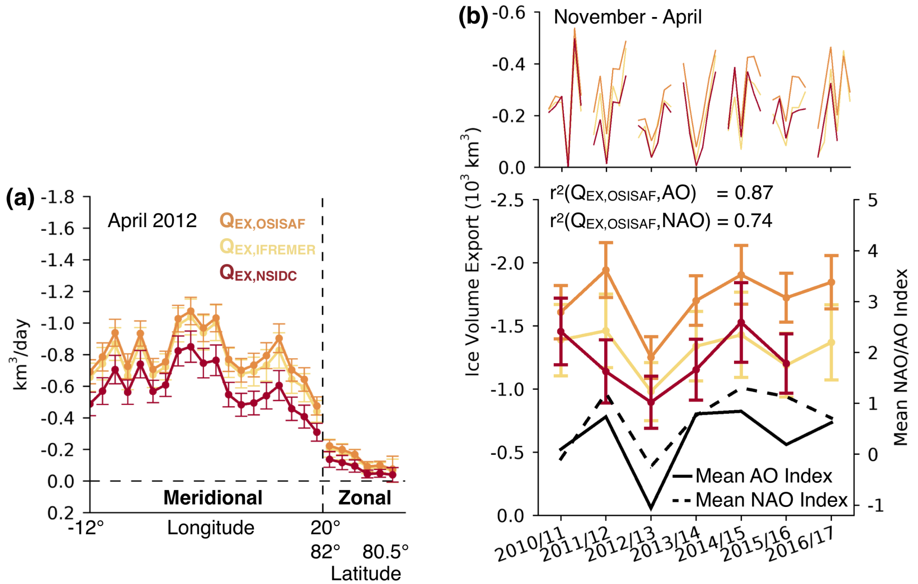

Figure 7. (a) Example for monthly ice volume export through the Fram Strait gate (April 2012) derived from three different ice drift products. (b) ~~Total~~ Monthly sea ice volume export (upper panel), and total Arctic ~~sea-ice~~ sea ice volume export through the Fram Strait for winter seasons 2010/2011 - 2016/2017, added together over the November-April period and derived from three different ice drift products (lower panel). Mean Arctic Oscillation (AO) Index and mean North Atlantic Oscillation Index (NAO) are shown for the same period, including coefficients of determination (r^2).

variations ~~with the minimum in 2012/2013~~ and the magnitudes of spatial gradients are similar for all products. Considering the correlation coefficients (r) between the monthly volume export retrievals (Figure 7b, upper panel), we find r($Q_{\mathrm{Ex,OSISAF}}$, $Q_{\mathrm{Ex,IFREMER}}$) = 0.94, r($Q_{\mathrm{Ex,OSISAF}}$, $Q_{\mathrm{Ex,NSIDC}}$) = 0.92 and $Q_{\mathrm{Ex,NSIDC}}$) = 0.90. Therefore, the choice of the drift products has no major impact on our export variability analysis. We also note, that it is not within the scope of this work to determine which product provides the most accurate estimate of sea ice drift in the Fram Strait.

4 Discussion

4.1 Relative contribution of sea ice drift, thickness and concentration to the volume flux variability

In order to understand the mechanisms behind the variability in ice volume export, we now examine the three input parameters, ice drift, thickness and concentration, in more detail. As shown in section 3.1, the thickness averaged across Fram Strait exhibits significant interannual changes with an overall increase in spring. This increase at the gate from autumn to spring can be associated with the thermodynamic ice growth and deformation of FYI and thin second-year ice. For example, ~~In~~ in 2011/2012 and 2013/2014, thickness of FYI grid cells rises from October to April (Figure 2). In contrast, in 2016/2017, the fraction of FYI passing the gate is only 6 %, and consequently, we do not observe significant changes in mean ice thickness during the

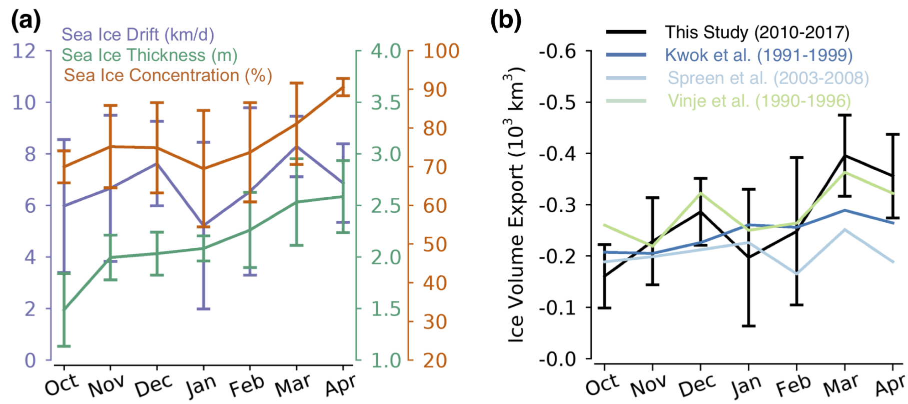

Figure 8. (a) Mean monthly sea ice drift, thickness and concentration at the Fram Strait gate over the years 2010/2011 - 2016/2017 with corresponding standard deviations. (b) Mean monthly ice volume export through the Fram Strait from this study, and from Spreen et al. (2009), Kwok et al. (2004), and Vinje et al. (1998) covering different periods.~~(b)~~

OA period. Similarly, we observe an increase in mean ice concentration at the gate during the OA period. Considering the ice drift, we find opposite features. The mean monthly drift in the time domain is highly variable, without a distinct trend over the OA period (Figure ~~7~~8a). These characteristics of the variability of input parameters affect the mean monthly ice volume export (Figure ~~7~~8b). The mean seasonal cycle over the period 2010-2017 is characterized by minimums in October and January and the maximum in March. Considering seasonal cycles of drift, thickness, and concentration at the gate and comparing it with the seasonal cycle of the ice export, we find that the variability is mostly explained by the ice drift (Figure ~~7~~8a) as also suggested by the RSD. On the other hand, the positive gradient of the ice volume export between autumn and spring with the annual maximum in March can be associated with the seasonal cycle of sea ice thickness (Figure ~~7~~8a). This seems primarily driven by thermodynamic ice growth and deformation. Although the seasonal cycle of mean ice concentration along the entire gate shows positive gradients as well, with a similar RSD as the ice thickness, it seems to play a minor role for the ice export variability. This is because ice concentration variability at the meridional gate is small due to the persistent ice coverage over the season. Considered separately, we find a RSD of 0.78 at the zonal gate and a RSD of 0.08 at the meridional gate. But due to the smaller size, lower ice drift and thinner ice, the zonal volume flux is only about 4 % of the total ice export over the 7-years period.

4.2 Comparison to previous studies

~~Sea-ice~~ sea ice export through the Fram Strait and its variability has been the focus of several previous studies. A major difference in the method is the choice of the position of the gate. Smedsrud et al. (2017) placed the gate at 79°N, Spreen et al. (2009) placed their most northern gate at 80°N, and Kwok and Rothrock (1999) placed their gate at about 81°N. Except for the study of Krumpen et al. (2016), all these previous studies use only a meridional gate or a straight connection between Greenland and Spitsbergen. The major advantage of using a gate positioned further north like at 82°N is that ice motion products and thickness estimates from satellites show lower uncertainties at this latitude. Indeed, errors and biases of low resolution ice drift data derived from passive microwave and scatterometer data become larger as ice velocity increases, and velocity tends to be larger with steeper gradients south of 82°N (Sumata et al., 2014, 2015). ~~On the other hand~~In addition, uncertainty of CS2 ice thickness increases at lower latitudes, especially in Fram Strait due to sparse orbit coverage (Ricker et al., 2014, 2017b). Therefore, we followed the approach of Krumpen et al. (2016), placing the gate at 82°N, which appears to be a good ~~compromise~~ choice in order to reduce uncertainty associated with our ice volume export estimate.

Figure ~~7~~8b shows the mean monthly winter export from October to April from this study, compared to previous estimates (Kwok et al., 2004; Spreen et al., 2009; Vinje et al., 1998). Vinje et al. (1998) and Kwok et al. (2004) use upward-looking sonar (ULS) data for the estimation of ice thickness in the Fram Strait. Vinje et al. (1998) use ULS ice draft measurements from 1990-1996 in combination with buoy and SAR-based ice drift estimates, and estimate ice volume fluxes through the Fram Strait that show maxima of up to about -600 km^3/month. Kwok et al. (2004) investigated nearly the same period (1991-1999) and find a maximum monthly export of -509 km^3/month in December 1994. Their estimates are generally lower than in Vinje et al. (1998). Spreen et al. (2009) use ice thickness and drift estimates derived from satellite data to compute ice volume flux, and therefore, their study is methodically similar to our work. However, besides the different gate at 80°N, they use a different ice thickness retrieval (ICESat) and another low resolution ice drift data set (Cersat/Ifremer, AMSR-E) to derive ice volume export. For the period 2003-2008, they estimate monthly winter ice volume export ranging from -100 to -420 km^3/month, using ULS ice thickness estimates to complement the two month-long ICESat measurement periods per year. The largest difference of about 150 km^3 between the lowest and largest estimate is found in March. Our estimate seems to be the one with the highest change between October and April, e.g. our estimates are the lowest in October, and the highest in April (Figure ~~7~~8b). Our seasonal cycle also reveals higher variability. Several factors might cause this discrepancy:

1. The observing periods are not overlapping and therefore, differences in mean monthly export can be caused by natural variations in ice thickness and drift.

2. Bottom melt due to the recirculation of warm Atlantic water between between 82°N and 80°N might lead to a reduction in ice volume (Wekerle et al., 2017).

3. The low resolution of the drift data might lead to systematic uncertainties in the volume flux at the gate, especially near the coast and the ice margins, affecting all retrievals.

4. Systematic differences between the CS2 and ICESat ice thickness retrievals may appear because of different retrieval algorithms and different sensor characteristics.

5. Ice drift at 80°N might be underestimated due large ice velocities, which are not well captured in radiometer- and scatterometer-based drift products.

Despite these differences, estimates from different studies exhibit consistent features, such as the maximum in March. In the following, we will discuss the interannual variability and the role of atmospheric circulation patterns.

4.3 Interannual ice volume export variability

The time series of winter ice volume export through the Fram Strait reveals a significant decrease of 500 km^3 from 2011/2012 to 2012/2013 (Figure ~~6~~7). This decrease is characterized by a drop of both the mean ice drift and the thickness through Fram Strait. Comparing the pan Arctic ice condition in both winters, a decrease of ice thickness north of Fram Strait has been reported for 2012/2013 by Ricker et al. (2017a), and was found to be mainly a result of anomalous summer melt and late freeze up in 2012. The ice in the area north of Fram Strait is the main source of exported ice (Smedsrud et al., 2017) and thus, we also find a drop in ice thickness at the Fram Strait for 2012/2013, which is accompanied by a lower mean drift (Figure ~~4~~5). In contrast, in winter season 2013/2014, which followed a cold Arctic summer with low melt rates (Tilling et al., 2015), ice thickness at the gate is increasing, accompanied by a higher mean drift (Figure ~~4~~5). This results in an ice volume export comparable to 2010/2011 (Figure ~~6~~7).

We also examine the link between ice volume export and North Atlantic Oscillation (NAO) index and the Arctic Oscillation (AO) index (Figure ~~6~~7b). The NAO index is defined as the sea level pressure anomaly between Lisbon, Portugal, and Reykjavik, Iceland. A positive NAO index is associated with an Icelandic low and a corresponding high-pressure system over the Azores. When the Icelandic low is intensified, the sea level pressure gradient in the Fram Strait increases, leading to strong northerly winds and hence, increased sea ice drift ~~(Kwok and Rothrock, 1999; Ionita et al., 2016; Smedsrud et al., 2017)~~(Kwok and Rothrock, 1999; Thus, a high, positive NAO index is associated with high ice volume export rates, since ice drift primarily drives the ice volume export variability. If both pressure systems are weak or even reversed, the NAO phase becomes negative and correlation between NAO and sea level pressure gradient along the Fram Strait decreases. The variability of the NAO is largest during the winter season. We have obtained monthly NAO indices from the National Oceanic and Atmospheric Administration (NOAA) and averaged them over the NA period. Positive phases (>1) of the NAO index occurred in 2011/2012 and 2014/2015, coinciding with increased mean monthly ice volume export rates (Figure ~~6~~7b).

The sea level pressure gradient variability through the Fram Strait is also captured in the AO and its corresponding index, described in Thompson and Wallace (1998). The AO pattern involves an oscillation of the sea level pressure between the Arctic basin and the surrounding zonal belt. The AO therefore includes characteristics of the NAO, which is regionally bounded. We have obtained monthly AO indices from NOAA (http://www.cpc.ncep.noaa.gov) and averaged them over the NA period. The variability of the AO index is similar to the variability of the NAO index and the ice volume export, especially if the flux is computed with IFREMER and OSISAF ice drift (Figure ~~6~~7b). The correlation between ice export and AO index ($r^2 = 0.87$) is larger than with the NAO index ($r^2 = 0.74$). This is because the NAO index decreases is 2016/2017, while the ice volume export increases compared to the previous year. However, we acknowledge that a longer time series is required to obtain statistical meaningful correlation coefficients.

4.4 The impact of ice volume export on Arctic ice mass balance

Kwok et al. (1999) investigated the area balance of the Arctic Ocean perennial ice zone between October 1996 and April 1997. Using RADARSAT data, they reported that winter MYI area loss can be explained almost entirely by ice export. Moreover,

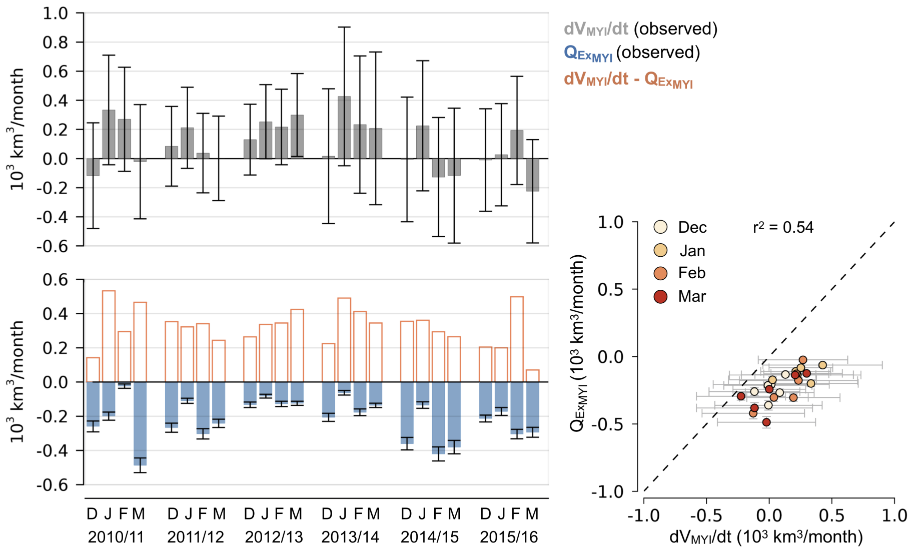

Figure 9. Monthly sea-ice MYI volume export through the Fram Strait (Q_{Ex} $Q_{\mathrm{Ex}_{\mathrm{MYI}}}$) and simultaneous Arctic sea-ice MYI volume growth rates (dV/dt dV_{MYI}/dt) between December and March for the winter seasons 2010/2011 - 2015/2016, divided into first-year ice (FYI) and multiyear ice (MYI). 2016. Error bars represent the corresponding uncertaintiesand blue and red lines represent the means over the December-March period. Scattergrams show The scattergram shows the relation between dV/dt dV_{MYI}/dt and Q_{Ex} $Q_{\mathrm{Ex}_{\mathrm{MYI}}}$, and corresponding coefficient of determination (r^2).

their findings suggest that export is dominated by ice flux through the Fram Strait, while export through other gates like Nares Strait plays a minor role. According to Kwok et al. (1999), MYI area export through Nares Strait is about 5 % of the Fram Strait MYI area export. The balance of MYI area is only affected by export and ice dynamics, assuming that the net melt of MYI area is zero in winter. As a consequence, Arctic MYI area is decreasing from October to April, and in turn, this decrease is almost entirely balanced by exported MYI area (Kwok et al., 1999).

In the following, we investigate the ice volume balance of the Arctic MYI. In contrast to MYI area, we assume that MYI volume growth rate of the Arctic Ocean domain (dV_{MYI}/dt) is affected by both export ($Q_{\mathrm{Ex}_{\mathrm{MYI}}}$) and ice volume gain due to thermodynamic growth ($dV_{\mathrm{therm}_{\mathrm{MYI}}}/dt$). Neglecting net melt of MYI in winter, we can write:

$$\frac{dV_{\mathrm{MYI}}}{dt} = Q_{\mathrm{Ex}_{\mathrm{MYI}}} + \left(\frac{dV_{\mathrm{therm}_{\mathrm{MYI}}}}{dt} + \frac{dV_{\mathrm{resid}_{\mathrm{MYI}}}}{dt}\right). \tag{9}$$

The term $dV_{\mathrm{resid}_{\mathrm{MYI}}}/dt$ accounts for residual contributions, such as . This includes ice deformation that might change the bulk ice density, which we assume to be constant. However, we believe that Moreover, new forming openings within the MYI zone due to divergence can bias the ice type classification when such areas are erroneously classified as MYI. This effect leads to a positive bias of dV_{MYI}/dt. A quantitative separation between $dV_{\mathrm{resid}_{\mathrm{MYI}}}/dt$ is small compared to and $dV_{\mathrm{therm}_{\mathrm{MYI}}}/dt$ is difficult. Therefore, we assume that winter MYI volume variability is primarily affected by changes in ice volume export and thermodynamic growth. only consider the entire contribution of the second term in Eq. (9).

We estimate monthly Arctic ~~FYI volume growth dV_{FYI}/dt and monthly Arctic~~ MYI volume growth ~~(~~dV_{MYI}/dt ~~)~~ by a 3-point Lagrangian interpolation scheme, where we exclude all ice south of the Fram Strait gate. Since CS2 ice thickness data are not available in October 2010, we compute ~~dV_{FYI}/dt and~~ dV_{MYI}/dt using data over the NA period and therefore obtain ~~dV_{FYI}/dt and~~ dV_{MYI}/dt values for December to March. Figure ~~8 shows monthly dV_{FYI}/dt (~~9 shows monthly dV_{MYI}/dt ~~) and corresponding $Q_{\mathrm{Ex}_{\mathrm{FYI}}}$ (~~and corresponding $Q_{\mathrm{Ex}_{\mathrm{MYI}}}$ ~~)~~ for 6 years. ~~Export has no significant impact on FYI volume variability, because the variability is dominated by the gain due to thermodynamic ice growth, which is up to 15 times higher than $Q_{\mathrm{Ex}_{\mathrm{FYI}}}$. The Scattergram in Figure 8 reveals the seasonal cycle of dV_{FYI}/dt, with a decrease of ice growth from December to March.~~ In addition, it shows the residual ($dV_{\mathrm{resid}_{\mathrm{MYI}}}/dt + dV_{\mathrm{therm}_{\mathrm{MYI}}}/dt$), which is not directly observed, but deduced by subtracting $Q_{\mathrm{Ex}_{\mathrm{MYI}}}$ from dV_{MYI}/dt. Winter season 2016/2017 is excluded here due to erroneous MYI ice classification, which affects dV_{MYI}/dt and $Q_{\mathrm{Ex}_{\mathrm{MYI}}}$ (Section 2.3).

MYI volume growth dV_{MYI}/dt does not follow a seasonal cycle as it is the case for FYI volume growth ~~dV_{FYI}/dt~~ that is primarily driven by the thermodynamic ice growth (Ricker et al., 2017a). ~~Our estimated dV_{FYI}/dt is in the order of 10 times higher than MYI volume growth dV_{MYI}/dt. This is a result of the thicker MYI associated with reduced thermodynamic ice growth on the one hand, and new forming ice as well as faster growing FYI on the other hand.~~ It appears that $Q_{\mathrm{Ex}_{\mathrm{MYI}}}$ is just in the range to almost or entirely balance the volume gain of the second term in Eq. (9), (~~$dV_{\mathrm{therm}_{\mathrm{MYI}}}/dt$ +~~ $dV_{\mathrm{resid}_{\mathrm{MYI}}}/dt$ + $dV_{\mathrm{therm}_{\mathrm{MYI}}}/dt$). For example, in 2014/2015 and 2015/2016, mean dV_{MYI}/dt is nearly zero due to ~~a~~ large $Q_{\mathrm{Ex}_{\mathrm{MYI}}}$ between December and March. ~~As a consequence~~It is possible that $Q_{\mathrm{Ex}_{\mathrm{MYI}}}$ exceeds $dV_{\mathrm{therm}_{\mathrm{MYI}}}/dt$, leading to a net reduction of Arctic MYI volume when considering a positive bias due to erroneous MYI type classification. However, the variability of dV_{MYI}/dt is significantly driven by $Q_{\mathrm{Ex}_{\mathrm{MYI}}}$, revealing a coefficient of determination (r^2) of 0.54, which means that 54 % of dV_{MYI}/dt during winter can be explained by variations of $Q_{\mathrm{Ex}_{\mathrm{MYI}}}$, assuming a linear relationship. From that, we can deduce that the variability of dV_{MYI}/dt is significantly driven by the variability of the ice drift in the Fram Strait.

The high correlation (0.74) between $Q_{\mathrm{Ex}_{\mathrm{MYI}}}$ and dV_{MYI}/dt is also noticeable. This proves the accuracy of Arctic MYI volume estimates as the correlation between $Q_{\mathrm{Ex}_{\mathrm{MYI}}}$ and dV_{MYI}/dt exposes the signal of ice volume export in the MYI volume budget. In case of large errors in dV_{MYI}/dt as indicated in Figure ~~8~~ 9 by the error bars, correlation with $Q_{\mathrm{Ex}_{\mathrm{MYI}}}$ would be degraded.

5 Conclusions

Here we have used, for the first time, the CryoSat-2 ice thickness retrievals in order to quantify the sea ice export through Fram Strait. We performed a detailed analysis of variability and important processes for the Arctic multiyear ice (MYI) mass balance. Based on our analysis, the following conclusions can be drawn:

1. Based on different ice drift products, the three ice volume export retrievals ($Q_{\mathrm{Ex,OSISAF}}$, $Q_{\mathrm{Ex,IFREMER}}$, $Q_{\mathrm{Ex,NSIDC}}$) exhibit similarities in their variability (correlations r>0.9), although they differ in magnitude by -23 % ($Q_{\mathrm{Ex,IFREMER}}$) and -26 % ($Q_{\mathrm{Ex,NSIDC}}$), compared to $Q_{\mathrm{Ex,OSISAF}}$. In order to investigate long-term trends in ice volume export derived from multiple satellite observations, we therefore need to construct multi-sensor consistent time series of ice drift,

thickness, and concentration. Moreover, a consistent methodology to compute ice volume flux through Fram Strait is required.

2. Ice drift shows coherent spatial variability across Fram Strait, but high frequency variability from month to month. The mean monthly ice drift across Fram Strait shows a peak at about 6°W, which could be associated with the East Greenland Current.

3. The relative standard deviation (RSD) is a measure to compare the variability of different physical quantities. At the Fram Strait gate, RSD of ice drift (0.37) is roughly twice as high as the RSD of ice thickness (0.19) and concentration (0.16) for the observation period of 2010/2011-2016/1017, revealing that ice drift is the main driver of seasonal and interannual variability of ice volume export. However, the seasonal trend of ice volume export is driven by variations in ice thickness due to the thermodynamic growth that typically leads to a maximum in March. Ice concentration variability is large at the zonal gate (RSD = 0.78), but small at the meridional gate (RSD = 0.08), where 96 % of the sea ice is exported.

4. Monthly sea-ice volume export through Fram Strait varies between -21 and -540 km^3/month.

5. The interannual variations of ice volume export can be explained by large scale variability of the atmospheric circulation captured by the Arctic Oscillation ($r^2 = 0.87$) and North Atlantic Oscillation indices ($r^2 = 0.74$).

6. While the seasonal cycle of Arctic first-year ice volume is driven by thermodynamic ice growth, 54 % of the ~~variability of~~ changes in Arctic MYI volume over the December-March period can be explained by ice volume export through the Fram Strait.

7. ~~While MYI area declines during the seasonal cycle, MYI volume is in equilibrium or slightly increases. We believe that this is a consequence of thermodynamic ice growth, which compensates the loss due to ice export. Contrary, MYI area loss due to export adds to the loss by area compression due to convergence.~~

Data availability. Sea ice concentration, sea ice type and sea ice drift data are provided by OSISAF (http://osisaf.met.no). CryoSat-2 ice thickness data from 2010-2017 are provided by http://www.meereisportal.de. IFREMER ice drift data from 2010 to 2017 are provided via CERSAT (http://cersat.ifremer.fr). NSIDC ice drift data from 2010 to 2015 are provided via https://nsidc.org.

Author contributions. Robert Ricker conducted the ice volume flux calculations and the analysis. Fanny Girard-Ardhuin, Thomas Krumpen and Camille Lique contributed to the analysis of the ice volume flux data. Robert Ricker wrote the paper and all Co-authors contributed to the discussion and gave input for writing.

Competing interests. The authors declare no conflict of interest.

Acknowledgements. This work has been conducted in the framework of the project: Space-borne observations for detecting and forecasting sea ice cover extremes (SPICES) funded by the European Union (H2020) (Grant: 640161). CryoSat-2 data are provided by http://www.meereisportal.de (Grant REKLIM-2013-04). Moreover, this work was supported by the German Ministry for Science and Education under Grant 03F0777A (QUARCCS) and the CORESAT project funded by the Norwegian Research Council (grant 222681).

References

Aaboe, S., Breivik, L.-A., Sørensen, A., Eastwood, S., and Lavergne, T.: Global sea ice edge and type product user's manual, OSI-403-c & EUMETSAT, 2016.

Alexandrov, V., Sandven, S., Wahlin, J., and Johannessen, O. M.: The relation between sea ice thickness and freeboard in the Arctic, The Cryosphere, 4, 373–380, https://doi.org/10.5194/tc-4-373-2010, http://www.the-cryosphere.net/4/373/2010/, 2010.

Comiso, J. C.: Arctic multiyear ice classification and summer ice cover using passive microwave satellite data, Journal of Geophysical Research: Oceans, 95, 13 411–13 422, https://doi.org/10.1029/JC095iC08p13411, http://dx.doi.org/10.1029/JC095iC08p13411, 1990.

de Steur L., E., H., R., G., M., K., E., F., and J., H.: Freshwater fluxes in the East Greenland Current: A decade of observations, Geophysical Research Letters, 36, https://doi.org/10.1029/2009GL041278, https://agupubs.onlinelibrary.wiley.com/doi/abs/10.1029/2009GL041278, 2009.

Dickson, R. R., Meincke, J., Malmberg, S.-A., and Lee, A. J.: The "great salinity anomaly" in the Northern North Atlantic 1968–1982, Progress in Oceanography, 20, 103 – 151, https://doi.org/https://doi.org/10.1016/0079-6611(88)90049-3, http://www.sciencedirect.com/science/article/pii/0079661188900493, 1988.

Eastwood, S.: OSI SAF Sea Ice Product Manual, v3.8 edn., http://osisaf.met.no, 2012.

Ezraty, R., Girard-Ardhuin, F., and Piollé, J.-F.: Sea ice drift in the central Arctic estimated from SeaWinds/QuikSCAT backscatter maps, User's Manual. Laboratoire d'Océanographie Spatiale(Département d'Océanographie Physique et Spatiale), IFREMER, Brest, 2007.

Girard-Ardhuin, F. and Ezraty, R.: Enhanced Arctic Sea Ice Drift Estimation Merging Radiometer and Scatterometer Data, IEEE Transactions on Geoscience and Remote Sensing, 50, 2639–2648, https://doi.org/10.1109/TGRS.2012.2184124, ftp://ftp.ifremer.fr/ifremer/cersat/products/gridded/psi-drift/, 2012.

Helm, V., Humbert, A., and Miller, H.: Elevation and elevation change of Greenland and Antarctica derived from CryoSat-2, The Cryosphere, 8, 1539–1559, https://doi.org/10.5194/tc-8-1539-2014, http://www.the-cryosphere.net/8/1539/2014/, 2014.

Hendricks, S., Ricker, R., and Helm, V.: User Guide - AWI CryoSat-2 Sea Ice Thickness Data Product (v1.2), hdl:10013/epic.48201, 2016.

Holland, M. M., Bitz, C. M., and Tremblay, B.: Future abrupt reductions in the summer Arctic sea ice, Geophysical Research Letters, 33, https://doi.org/10.1029/2006GL028024, http://dx.doi.org/10.1029/2006GL028024, 2006.

Ionita, M., Scholz, P., Lohmann, G., Dima, M., and Prange, M.: Linkages between atmospheric blocking, sea ice export through Fram Strait and the Atlantic Meridional Overturning Circulation, Scientific Reports, 6, 32 881 EP –, http://dx.doi.org/10.1038/srep32881, 2016.

Ivanova, N., Johannessen, O. M., Pedersen, L. T., and Tonboe, R. T.: Retrieval of Arctic Sea Ice Parameters by Satellite Passive Microwave Sensors: A Comparison of Eleven Sea Ice Concentration Algorithms, IEEE Transactions on Geoscience and Remote Sensing, 52, 7233–7246, https://doi.org/10.1109/TGRS.2014.2310136, 2014.

Krumpen, T., Gerdes, R., Haas, C., Hendricks, S., Herber, A., Selyuzhenok, V., Smedsrud, L., and Spreen, G.: Recent summer sea ice thickness surveys in Fram Strait and associated ice volume fluxes, The Cryosphere, 10, 523–534, https://doi.org/10.5194/tc-10-523-2016, http://www.the-cryosphere.net/10/523/2016/, 2016.

Kwok, R.: Near zero replenishment of the Arctic multiyear sea ice cover at the end of 2005 summer, Geophysical Research Letters, 34, https://doi.org/10.1029/2006GL028737, http://dx.doi.org/10.1029/2006GL028737, 2007.

Kwok, R. and Cunningham, G.: Variability of Arctic sea ice thickness and volume from CryoSat-2, Philosophical Transactions of the Royal Society of London A: Mathematical, Physical and Engineering Sciences, 373, 20140 157, 2015.

Kwok, R. and Rothrock, D. A.: Variability of Fram Strait ice flux and North Atlantic Oscillation, Journal of Geophysical Research: Oceans, 104, 5177–5189, https://doi.org/10.1029/1998JC900103, http://dx.doi.org/10.1029/1998JC900103, 1999.

Kwok, R., Cunningham, G. F., and Yueh, S.: Area balance of the Arctic Ocean perennial ice zone: October 1996 to April 1997, Journal of Geophysical Research: Oceans, 104, 25 747–25 759, https://doi.org/10.1029/1999JC900234, http://dx.doi.org/10.1029/1999JC900234, 1999.

Kwok, R., Cunningham, G. F., and Pang, S. S.: Fram Strait sea ice outflow, Journal of Geophysical Research: Oceans, 109, n/a–n/a, https://doi.org/10.1029/2003JC001785, http://dx.doi.org/10.1029/2003JC001785, c01009, 2004.

Lavergne, T., Eastwood, S., Teffah, Z., Schyberg, H., and Breivik, L.-A.: Sea ice motion from low-resolution satellite sensors: An alternative method and its validation in the Arctic, Journal of Geophysical Research: Oceans, 115, n/a–n/a, https://doi.org/10.1029/2009JC005958, http://dx.doi.org/10.1029/2009JC005958, c10032, 2010.

Laxon, S., Peacock, N., and Smith, D.: High interannual variability of sea ice thickness in the Arctic region, Nature, 425, 947–950, 2003.

Laxon, S. W., Giles, K. A., Ridout, A. L., Wingham, D. J., Willatt, R., Cullen, R., Kwok, R., Schweiger, A., Zhang, J., Haas, C., Hendricks, S., Krishfield, R., Kurtz, N., Farrell, S., and Davidson, M.: CryoSat-2 estimates of Arctic sea ice thickness and volume, Geophysical Research Letters, 40, 732–737, https://doi.org/10.1002/grl.50193, http://dx.doi.org/10.1002/grl.50193, 2013.

Lique, C., Treguier, A. M., Scheinert, M., and Penduff, T.: A model-based study of ice and freshwater transport variability along both sides of Greenland, Climate Dynamics, 33, 685–705, https://doi.org/10.1007/s00382-008-0510-7, https://doi.org/10.1007/s00382-008-0510-7, 2009.

Maslanik, J., Stroeve, J., Fowler, C., and Emery, W.: Distribution and trends in Arctic sea ice age through spring 2011, Geophysical Research Letters, 38, https://doi.org/10.1029/2011GL047735, http://dx.doi.org/10.1029/2011GL047735, 2011.

Parkinson, C. L. and Comiso, J. C.: On the 2012 record low Arctic sea ice cover: Combined impact of preconditioning and an August storm, Geophysical Research Letters, 40, 1356–1361, https://doi.org/10.1002/grl.50349, http://dx.doi.org/10.1002/grl.50349, 2013.

R., K., G., S., and S., P.: Arctic sea ice circulation and drift speed: Decadal trends and ocean currents, Journal of Geophysical Research: Oceans, 118, 2408–2425, https://doi.org/10.1002/jgrc.20191, https://agupubs.onlinelibrary.wiley.com/doi/abs/10.1002/jgrc.20191, 2013.

Ricker, R., Hendricks, S., Helm, V., Skourup, H., and Davidson, M.: Sensitivity of CryoSat-2 Arctic sea-ice freeboard and thickness on radar-waveform interpretation, The Cryosphere, 8, 1607–1622, https://doi.org/10.5194/tc-8-1607-2014, http://www.the-cryosphere.net/8/1607/2014/, 2014.

Ricker, R., Hendricks, S., Girard-Ardhuin, F., Kaleschke, L., Lique, C., Tian-Kunze, X., Nicolaus, M., and Krumpen, T.: Satellite-observed drop of Arctic sea ice growth in winter 2015–2016, Geophysical Research Letters, 44, 3236–3245, https://doi.org/10.1002/2016GL072244, http://dx.doi.org/10.1002/2016GL072244, 2016GL072244, 2017a.

Ricker, R., Hendricks, S., Kaleschke, L., Tian-Kunze, X., King, J., and Haas, C.: A weekly Arctic sea-ice thickness data record from merged CryoSat-2 and SMOS satellite data, The Cryosphere, 11, 1607–1623, https://doi.org/10.5194/tc-11-1607-2017, https://www.the-cryosphere.net/11/1607/2017/, 2017b.

Rudels, B., Fahrbach, E., Meincke, J., Budéus, G., and Eriksson, P.: The East Greenland Current and its contribution to the Denmark Strait overflow, ICES Journal of Marine Science, 59, 1133–1154, https://doi.org/10.1006/jmsc.2002.1284, +http://dx.doi.org/10.1006/jmsc.2002.1284, 2002.

Smedsrud, L. H., Halvorsen, M. H., Stroeve, J. C., Zhang, R., and Kloster, K.: Fram Strait sea ice export variability and September Arctic sea ice extent over the last 80 years, The Cryosphere, 11, 65–79, https://doi.org/10.5194/tc-11-65-2017, https://www.the-cryosphere.net/11/65/2017/, 2017.

Spreen, G., Kern, S., Stammer, D., and Hansen, E.: Fram Strait sea ice volume export estimated between 2003 and 2008 from satellite data, Geophysical Research Letters, 36, n/a–n/a, https://doi.org/10.1029/2009GL039591, http://dx.doi.org/10.1029/2009GL039591, l19502, 2009.

Spreen, G., Kwok, R., and Menemenlis, D.: Trends in Arctic sea ice drift and role of wind forcing: 1992–2009, Geophysical Research Letters, 38, https://doi.org/10.1029/2011GL048970, http://dx.doi.org/10.1029/2011GL048970, l19501, 2011.

Stroeve, J. C., Markus, T., Boisvert, L., Miller, J., and Barrett, A.: Changes in Arctic melt season and implications for sea ice loss, Geophysical Research Letters, 41, 1216–1225, https://doi.org/10.1002/2013GL058951, http://dx.doi.org/10.1002/2013GL058951, 2013GL058951, 2014.

Sumata, H., Lavergne, T., Girard-Ardhuin, F., Kimura, N., Tschudi, M. A., Kauker, F., Karcher, M., and Gerdes, R.: An intercomparison of Arctic ice drift products to deduce uncertainty estimates, Journal of Geophysical Research: Oceans, 119, 4887–4921, https://doi.org/10.1002/2013JC009724, http://dx.doi.org/10.1002/2013JC009724, 2014.

Sumata, H., Gerdes, R., Kauker, F., and Karcher, M.: Empirical error functions for monthly mean Arctic sea-ice drift, Journal of Geophysical Research: Oceans, 120, 7450–7475, https://doi.org/10.1002/2015JC011151, http://dx.doi.org/10.1002/2015JC011151, 2015.

Thomas, D. R. and Rothrock, D. A.: The Arctic Ocean ice balance: A Kalman smoother estimate, Journal of Geophysical Research: Oceans, 98, 10 053–10 067, https://doi.org/10.1029/93JC00139, http://dx.doi.org/10.1029/93JC00139, 1993.

Thompson, D. W. J. and Wallace, J. M.: The Arctic oscillation signature in the wintertime geopotential height and temperature fields, Geophysical Research Letters, 25, 1297–1300, https://doi.org/10.1029/98GL00950, http://dx.doi.org/10.1029/98GL00950, 1998.

Tilling, R. L., Ridout, A., Shepherd, A., and Wingham, D. J.: Increased Arctic sea ice volume after anomalously low melting in 2013, Nature Geoscience, 8, 643–646, 2015.

Tilling, R. L., Ridout, A., and Shepherd, A.: Near-real-time Arctic sea ice thickness and volume from CryoSat-2, The Cryosphere, 10, 2003–2012, https://doi.org/10.5194/tc-10-2003-2016, http://www.the-cryosphere.net/10/2003/2016/, 2016.

Tonboe, R., Lavelle, J., Pfeiffer, R.-H., and Howe, E.: Product User Manual for OSI SAF Global Sea Ice Concentration, OSI-401-b & EUMETSAT, 2017.

Vinje, T., Nordlund, N., and Kvambekk, Å.: Monitoring ice thickness in Fram Strait, Journal of Geophysical Research: Oceans, 103, 10 437–10 449, https://doi.org/10.1029/97JC03360, http://dx.doi.org/10.1029/97JC03360, 1998.

Warren, S. G., Rigor, I. G., Untersteiner, N., Radionov, V. F., Bryazgin, N. N., Aleksandrov, Y. I., and Colony, R.: Snow depth on Arctic sea ice, Journal of Climate, 12, 1814–1829, 1999.

Wekerle, C., Wang, Q., Danilov, S., Schourup-Kristensen, V., von Appen, W.-J., and Jung, T.: Atlantic Water in the Nordic Seas: Locally eddy-permitting ocean simulation in a global setup, Journal of Geophysical Research: Oceans, 122, 914–940, https://doi.org/10.1002/2016JC012121, http://dx.doi.org/10.1002/2016JC012121, 2017.

Wingham, D., Francis, C., Baker, S., Bouzinac, C., Brockley, D., Cullen, R., de Chateau-Thierry, P., Laxon, S., Mallow, U., Mavrocordatos, C., Phalippou, L., Ratier, G., Rey, L., Rostan, F., Viau, P., and Wallis, D.: CryoSat: A mission to determine the fluctuations in Earth's land and marine ice fields, Advances in Space Research, 37, 841 – 871, https://doi.org/10.1016/j.asr.2005.07.027, 2006.

Satellite-derived sea ice export and its impact on Arctic ice mass balance

Robert Ricker[1,2], Fanny Girard-Ardhuin[2], Thomas Krumpen[1], and Camille Lique[2]

[1]Alfred Wegener Institute, Helmholtz Centre for Polar and Marine Research, Bremerhaven, Bussestrasse 24, 27570 Bremerhaven, Germany

[2]Univ. Brest, CNRS, IRD, Ifremer, Laboratoire d'Oceanographie Physique et Spatiale (LOPS), IUEM, 29280, Brest, France

Correspondence to: Robert Ricker (Robert.Ricker@awi.de)

Abstract. Sea ice volume export through the Fram Strait represents an important fresh water input to the North Atlantic, which could in turn modulate the intensity of the thermohaline circulation. It also contributes significantly to variations of Arctic ice mass balance. We present the first estimates of winter sea ice volume export through the Fram Strait using CryoSat-2 sea ice thickness retrievals and three different drift products for the years 2010 to 2017. The monthly export varies between -21 and -540 km^3. We find that ice drift variability is the main driver of annual and interannual ice volume export variability, and that the interannual variations of the ice drift are driven by large scale variability of the atmospheric circulation captured by the Arctic Oscillation and North Atlantic Oscillation indices. On shorter timescale, however, the seasonal cycle is also driven by the mean thickness of exported sea ice, typically peaking in March. Considering Arctic winter multiyear ice volume changes, 54 % of their variability can be explained by the variations of ice volume export through the Fram Strait.

1 Introduction

Variability of the Arctic sea ice export contributes significantly to the variations of surface salinity in the subpolar gyre, and in particular in the regions where deep convection occurs, such as the Labrador and Greenland Seas. Fram Strait ice export represents approximately 25% of the total fresh water export to the North Atlantic (Lique et al., 2009). By the impact on convective overturning of water masses in the North Atlantic, changes in the export rates could affect the global ocean thermohaline circulation (Dickson et al., 1988). A recent study by Ionita et al. (2016) reports that persistent atmospheric blocking in winter leads to increased sea ice export through the Fram Strait, causing abrupt shifts in the Atlantic meridional overturning circulation variability. In turn, this might also affect the climate over Europe.

Arctic sea ice volume and related interannual variations have been investigated for the winter season (October-April) in various recent studies, using satellite altimetry (Tilling et al., 2015; Kwok and Cunningham, 2015; Ricker et al., 2017a). While first-year sea ice (FYI) volume reveals a distinct seasonal cycle between October and April due to thermodynamic growth and new forming ice, multiyear sea ice (MYI) volume shows only small changes within this period (Ricker et al., 2017a).

MYI is defined as sea ice that survived at least one summer melt period. Its greater age implies that it went through a longer period of thermodynamic ice growth and additional thickening due to deformation. Therefore, MYI can reach several meters of thickness, making it resistant against melting and storms. Parkinson and Comiso (2013) have shown that storms like in August

2012 can cause a break up of the weakened ice surface, leading to a reduction of ice area. MYI attenuates potential loss of ice coverage due to external forcing, while the thinner FYI is much more sensitive to storms and temperature fluctuations (Holland et al., 2006). As a consequence, summer ice concentration strongly correlates with MYI coverage, highlighting its climate relevance (Comiso, 1990; Thomas and Rothrock, 1993). Maslanik et al. (2011) have shown that Arctic MYI fraction has been shrinking during the last decades, from about 75% in the mid 1980s to 45% in 2011. Indeed, anomalously large summer melt reduces the MYI volume and prevents its replenishment by aging FYI (Stroeve et al., 2014; Kwok, 2007).

The variability of the Arctic sea ice mass balance is determined by sea ice production and melt on the one hand, and sea ice export on the other hand. The Fram Strait represents the main Arctic gate for sea ice export. While ice export rates during summer are relatively low (Krumpen et al., 2016), winter ice export plays an important role for the MYI mass balance in the Arctic (Kwok et al., 1999). Therefore, in order to improve our understanding of these processes that are linked to the variability of Arctic MYI mass balance, monitoring winter sea ice volume export through the Fram Strait is crucial. Only satellite measurements have the capability to continuously monitor pan-arctic changes in ice concentration, thickness and drift, the parameters required for calculating ice volume flux. Spreen et al. (2009) estimated Fram Strait sea ice volume export between 2003 and 2008. They used ICESat laser altimeter observations to derive sea ice thickness and AMSR-E 89 GHz passive microwave data to retrieve sea ice concentration and drift. A comparison with previous estimates that were based on a parametrization of ice thickness (Vinje et al., 1998; Kwok and Rothrock, 1999) and drift (Vinje et al., 1998) did not indicate a significant change of the total amount of Fram Strait sea ice export between the 1990s and 2008. However, one needs to keep in mind that ICESat measurements were restricted to two periods per winter season, October/November and February/March. Thus, investigations on the seasonal cycle of ice volume export were limited. The European Space Agency (ESA) satellite CryoSat-2 (CS2) was launched in 2010 and partly overcomes these limitations (Wingham et al., 2006) as monthly Arctic wide CS2 sea ice thickness estimates are derived between October and April (Tilling et al., 2016; Ricker et al., 2014). This allows to produce unrivaled monthly estimates of ice volume export using satellite data and contributes to overarching objectives, such as the quantification of fresh water input from the Arctic to the subpolar North Atlantic, affecting the Atlantic meridional overturning circulation.

In this study, we pursue four main objectives. First, we use the Alfred Wegener Institute (AWI) CS2 ice thickness data set (Ricker et al., 2014) to estimate for the first time winter sea ice export through Fram Strait over 7 years between 2010 and 2017 (October-April) and compare our estimates with previous studies. We use three different low-resolution ice drift products in order to assess the impact of the chosen drift data set. Second, we aim to examine the temporal variability of volume export and its links with variability in sea ice drift, thickness and concentration. We then relate the interannual variability of ice volume export through Fram Strait to the variability of the atmospheric circulation captured by the Arctic Oscillation and North Atlantic Oscillation indices. Our fourth objective is to quantify the impact of winter ice volume export on Arctic sea ice mass balance, which will be achieved by considering Arctic net monthly ice volume changes.

The paper is organized as follows. Section 2 describes the CS2 ice thickness product, the used ice drift data and ancillary data sets. In section 3, we first examine spatial and temporal variability of sea ice thickness, drift and ice concentration at the

Table 1. Ice drift products used for this study.

Name	Product	Input data	Temporal resolution	Spatial resolution	Period
OSISAF	OSI-405 (merged)	SSMIS (91 GHz, DMSP F17), ASCAT (Metop-B), AMSR-2 (18.7 and 36.5 GHz)	48 h	62.5 km	2009 - 2017
IFREMER	CERSAT (merged)	QuikSCAT, ASCAT (MetOp-A , Metop-B), SSM/I (85 GHz), SSMIS (91 GHz)	1 month	62.5 km	1991 - 2017
NSIDC	Polar Pathfinder v3.0	AMSR-E (89 GHz), SSM/I (85 GHz), SMMR (37 GHz), AVHRR, buoy position, NCEP/NCAR wind data	1 month	25 km	1978 - 2017

Fram Strait gate and present estimates of the ice volume flux and Fram Strait export. The seasonal and interannual variability of ice volume export and its impact on Arctic ice mass balance are discussed in section 4. Conclusions are drawn in section 5.

2 Data and Methods

In this section, we describe data products used in this study, as well as methods to retrieve ice volume fluxes through the Fram Strait. Table 1 summarizes the specifications of the ice drift products. In addition to ice drift, also ice thickness and concentration data are required to estimate ice volume fluxes.

2.1 Sea Ice drift

2.1.1 OSI SAF

We use the low resolution sea ice drift data set from the Ocean and Sea Ice Satellite Application Facility (OSI SAF), specifically the OSI-405 multi sensor product. Various sensors and channels are processed in order to produce the merged product used here: SSMIS (91 GHz H&V polarization) on board DMSP platform F17, ASCAT (C-band backscatter) on board platform Metop-A, and AMSR-2 on board JAXA platform GCOM-W. Ice drift is estimated by an advanced cross-correlation method (Continuous Maximum cross-correlation (MCC)) on pairs of satellite images (Lavergne et al., 2010). The merged product considers the different single sensor data and their quality statistics in order to compensate for data gaps in the single sensor products. We use this multi sensor data set, since we require a sufficient data coverage in the Fram Strait area, which is not given by the single sensor products. Displacements and geographic coordinates of the start and end point of the displacements for 48 h time spans are provided on a 62.5 km x 62.5 km polar stereographic grid. In the following we refer to this product as *OSISAF*.

2.1.2 Ifremer

From Ifremer/CERSAT, we use the merged product, which is obtained from combining Advanced Scatterometer (ASCAT) data and special sensor microwave/imager (SSM/I) brightness temperature measurements. It is provided for different time spans, including monthly lags, which is suitable for our study. The algorithm to deduce ice drift from scatterometer data and the merging with radiometer data is described in Ezraty et al. (2007) and Girard-Ardhuin and Ezraty (2012). Geographic coordinates of the start and end point of the displacements are provided on a 62.5 km x 62.5 km polar stereographic grid. In the following we refer to this product as *IFREMER*.

2.1.3 NSIDC

Finally, we also use the Polar Pathfinder Sea Ice Motion Vectors (version 3), distributed by the National Snow and Ice Data Center (NSIDC). It provides a year-round ice drift data set. As for OSISAF and IFREMER, ice drift is obtained from multiple satellite sensors including radiometers and scatterometers (Table 1) complemented by buoy observations from the International Arctic Buoy Program (IABP). During summer, NCEP/NCAR winds speeds are used to estimate ice drift when satellite data are not available. Though we do not make use of the summer ice drift data, we choose to include this data set, since it is widely used in other studies (e.g. Krumpen et al. (2016) and Spreen et al. (2011)). Monthly Displacements in x and y direction are provided on an EASE 2 25 km x 25 km polar stereographic grid. In the following we refer to this product as *NSIDC*. In contrast to OSISAF and IFREMER, NSIDC is only available until February 2017, which means that we do not consider winter season 2016/2017 for NSIDC.

2.2 AWI CS2 sea ice thickness

We use the AWI CS2 product (processor version 1.2). Processing is based on CS2 orbit data files provided by ESA. Radar waveforms are processed according to Hendricks et al. (2016) and Ricker et al. (2014), using a 50% threshold-first-maximum retracker to obtain ellipsoidal surface elevations (Ricker et al., 2014; Helm et al., 2014). Radar waveforms from surfaces that contain openings in the ice pack appear as specular echoes and can be separated from diffuse echoes that contain reflections from sea ice only. Based on this surface type classification, open water elevations are identified and used to derive the instantaneous sea-surface height anomaly by interpolation. To retrieve sea ice freeboard, the sea-surface height anomaly is subtracted from the ice surface elevations.

Freeboard is converted into sea ice thickness by assuming hydrostatic equilibrium (Laxon et al., 2003). For the conversion, we use ice densities of 916.7 kg/m^3 and 882.0 kg/m^3 for FYI and MYI respectively (Alexandrov et al., 2010), and 1024 kg/m^3 for the sea water density. Snow depth and density are deduced from the Warren snow climatology (W99) (Warren et al., 1999). The climatology is modified by reducing the snow depth by 50 % over FYI to take into account the recent change towards a seasonal Arctic ice cover. FYI and MYI are identified with the daily OSI SAF sea ice type product (Eastwood, 2012). In order to obtain a sufficient spatial coverage, acquired thickness data are averaged monthly on an 25 km EASE 2 grid.

The CS2 observational uncertainties of sea ice thickness contain contributions that are associated with speckle noise, sea-surface height estimation, snow depth, and densities of ice and snow (Ricker et al., 2014). They can easily reach values of > 1 m for single measurements, but will be reduced to the range of centimeters by spatial averaging. Note that during the melting period from May to September, the presence of melt ponds prevents the retrieval of sea ice thickness observations.

2.3 OSI SAF Ice concentration and type

We use the sea ice concentration (OSI-401) and sea ice type product (OSI-403) of the European Organisation for the Exploitation of Meteorological Satellites (EUMETSAT) Ocean and Sea Ice Satellite Application Facility (OSI SAF). Ice concentration is computed from radiometer data, using a combination of state-of-the-art algorithms (Tonboe et al., 2017). Ice type is derived from passive microwave and active microwave scatterometer data combined in a Bayesian approach (Aaboe et al., 2016). Ice concentration is needed for the ice volume computation for each 25 km grid cell and ice type is used to classify grid cells as FYI or MYI. The products are updated daily and the data are provided on a 10 km polar stereographic grid. To be consistent with the CS2 product, monthly means are projected onto the EASE2 25 km grid. Ice type grid cells originally flagged as *ambiguous* are replaced by an inverse-distance interpolation to obtain FYI or MYI flags for all ice-covered grid cells. Errors can occur due to new forming openings within the MYI zone that are not captured and therefore classified as MYI. Especially in the Fram Strait, where floes can break up into many smaller pieces, this might lead to significant errors in MYI fraction. Moreover, we have observed erroneous MYI classification in the Arctic Basin during winter 2016/2017. The reason is not yet clear, but could to be a result of external factors such as exceptional warm winter temperatures. Therefore, FYI/MYI separation for 2016/2017 should be considered with caution (S. Aaboe, personal communication, 2017).

2.4 Retrieving ice volume flux and export rates through Fram Strait

The first step is to project the ice drift and thickness data onto a common grid. The EASE 2 grid is based on an equal area projection, and therefore, it is reasonable to use it for sea ice volume estimations (Ricker et al., 2017a). Hence, we define the 25 km EASE 2 grid provided in the AWI CS2 ice thickness product as our standard grid and interpolate the displacement data onto this grid. Since the NSIDC displacement data are already projected on an EASE grid, we only interpolate the displacements in x and y direction onto the 25 km grid. In contrast, the IFREMER and OSISAF grids are based on a polar stereographic projection. Here, we use the geographic coordinates of the start and end point of the displacement and project them onto the EASE 2 grid separately. Afterwards, displacements in x and y direction of the EASE 2 grid are calculated. Since the IFREMER and NSIDC products are provided as monthly means, the daily updated OSISAF 48 h displacements need to be summed up to monthly retrievals. Here, we calculate the displacements in x and y direction on the EASE 2 grid for each day and sum them up over one month.

Monthly ice volume flux $Q_{x,y}$ in x and y direction is obtained by:

$$Q_{xy} = lHCD_{xy}, \quad (1)$$

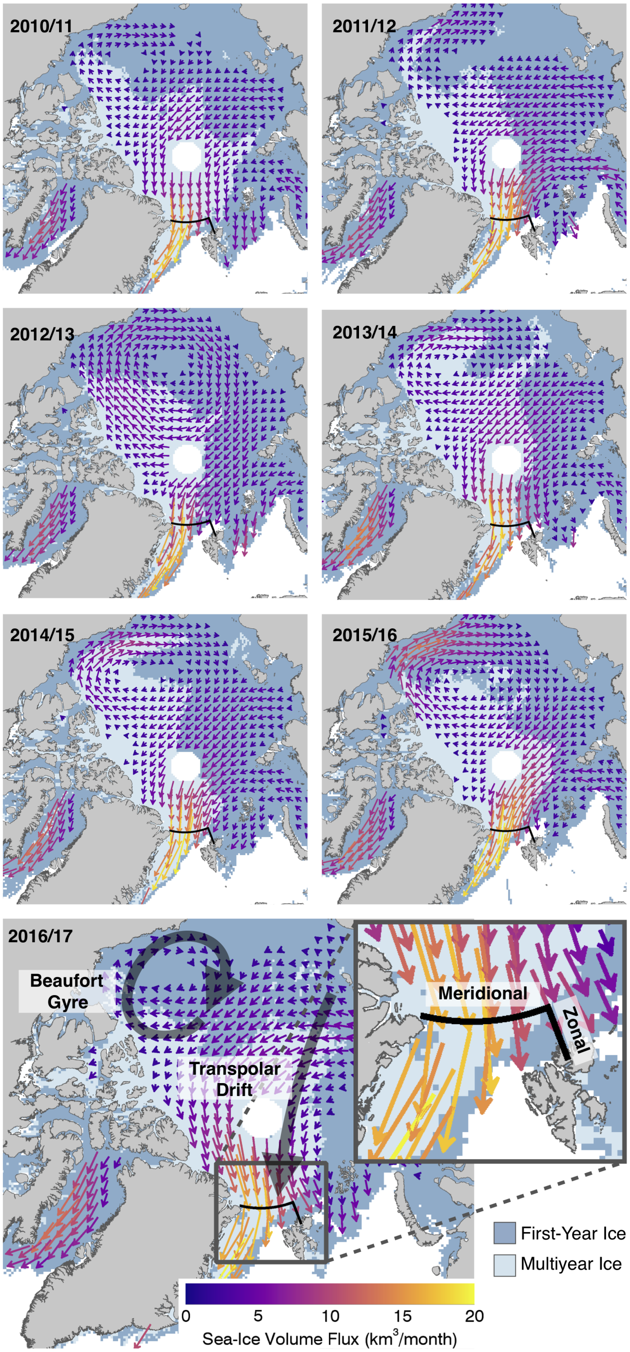

Figure 1. Means of Arctic sea ice volume fluxes for 2010/2011 - 2016/2017 between October and April. The enlarged box shows the location of the Fram Strait gate at 82°N, which is used for the calculation of the export rates, separated into meridional and zonal gates.

where l = 25 km is the size of the grid cells, H is the CS2 sea ice thickness, C is the ice concentration obtained from the OSISAF product, and D_{xy} represents the ice drift in x and y direction respectively.

In order to compute ice volume export through Fram Strait, we follow the methodology of Krumpen et al. (2016) and define a gate that is a composite of a meridional and a zonal gate (Figure 1). The meridional gate is located along 82°N between 12°W and 20°E. The zonal part is located along 20°E between 80.5°N and 82°N. We have chosen this gate location to reduce errors and biases in low resolution ice drift data that become larger with increasing ice velocities, typically found south of 82°N (Sumata et al., 2014, 2015). Moreover, uncertainty of CS2 ice thickness increases at lower latitudes, especially near Fram Strait due to sparse orbit coverage (Ricker et al., 2014).

Meridional components Q_{v} of the ice volume flux through the defined gate are calculated as follows:

$$
\begin{aligned}
Q_v &= l_{uv} H C D_v \\
Q_v &= l_{uv} H C (D_x \sin(\lambda) - D_y \cos(\lambda)).
\end{aligned}
\tag{2}
$$

The zonal components Q_{u} of the ice volume flux are computed accordingly:

$$
\begin{aligned}
Q_u &= l_{uv} H C D_u \\
Q_u &= l_{uv} H C (D_x \cos(\lambda) + D_y \sin(\lambda)),
\end{aligned}
\tag{3}
$$

where λ is the longitude of the respective grid cell and l_{uv} the length of the grid cell as a function of λ:

$$l_{uv} = l / \cos(\lambda) \tag{4}$$

Uncertainties of Q_v are estimated by:

$$\sigma_{Q_v} = l_{uv} \sqrt{(HC\sigma_D)^2 + (D_v C \sigma_H)^2 + (H D_v \sigma_C)^2}. \tag{5}$$

Meridional uncertainties σ_{Q_u} are calculated accordingly. Consistent with Laxon et al. (2013) and Ricker et al. (2017a), we set the ice-concentration uncertainty $\sigma_{\mathrm{c_i}}$ = 5%. Nevertheless, we acknowledge that the uncertainty may vary depending on the actual ice concentration (Ivanova et al., 2014). Sea ice thickness uncertainty σ_{H} is provided in the AWI CS2 ice thickness product (Ricker et al., 2014). Ice drift uncertainty σ_{D} is estimated using the empirical error functions for monthly mean Arctic sea ice drift given in Sumata et al. (2015), which utilizes drift estimates from high-resolution SAR data as a reference:

$$\sigma_D = \sqrt{\epsilon_x^2 + \epsilon_y^2}, \tag{6}$$

with the drift error functions $\epsilon_{x,y}$ in x and y direction of the grid used in Sumata et al. (2015):

$$\epsilon_{x,y} = \sqrt{\sigma_{x,y}^2 + \delta_{x,y}^2}, \tag{7}$$

where $\sigma_{x,y}$ are standard errors in x and y directions given in Sumata et al. (2015) for different categories of drift speed and ice concentration for each of the three drift products. Here, we use standard errors for the highest drift speed (> 4.3 km/d). $\delta_{x,y}$

represents the error of the reference drift data set, provided in Sumata et al. (2015). The deduced drift uncertainties for the low resolution drift products are in the range of 1.0 km/d, which is comparable to uncertainties estimated in previous studies (Spreen et al., 2009). These estimates do not include systematic errors. A comparison of different drift products in Sumata et al. (2014) shows significant systematic differences between the different drift products, especially for high drift speeds. Since we aim to investigate variabilities in ice volume export, we do not consider potential biases in this study.

We obtain the total ice volume flux through the Fram Strait (Q_{Ex}) by adding up the meridional zonal grid cell fluxes Q_v and Q_u along the gate:

$$Q_{\mathrm{Ex}} = \sum Q_u + \sum Q_v. \tag{8}$$

Note that following the axes conventions, ice volume export Q_{Ex} has a negative algebraic sign, corresponding to a sea ice loss from the Arctic Basin.

3 Results

In this section, we first examine sea ice drift, thickness and concentration at the Fram Strait gate. Throughout the study, we use the OSISAF drift as the reference product, because it shows the best performance among the used products in the Fram Strait (Sumata et al., 2014). Second, we present estimates of the ice volume flux in the Arctic and the calculated export through Fram Strait. Third, we examine the choice of the drift product, computing ice volume export using also IFREMER and NSIDC ice drift estimates. Throughout the paper, we refer to the winter period from October to April (OA). However, seasonal export estimates are calculated adding together monthly export from November to April (NA), since we have no ice thickness estimates for October 2010.

3.1 Sea ice drift, thickness and concentration at the gate

We consider all input parameters for Eq. (1), sea ice thickness (H), sea ice drift (D), and ice concentration (C). Figure 2 shows the spatiotemporal distribution of CS2 ice thickness along the meridional and zonal gates through each winter season, separated into FYI and MYI. Ice thickness along the gate is variable and ranges from 0 to 5 m. The mean gate thickness reveals a consistent gradient from thinner ice in October to thicker ice in April in all years, although the gradient can be small for some years (e.g. 2016/2017). Averaging over each OA period reveals the spatial thickness distribution along the meridional and zonal gates. In 2012/2013 and 2013/2014, we find a significant positive thickness gradient towards the coast of Greenland, while in other years, this is less pronounced. At the zonal gate, ice thickness decreases towards Svalbard. During winter seasons 2011/2012, 2012/2013 and 2013/2014, fraction of grid cells that contain MYI is lower compared to other years. In 2012/2013 and 2013/2014, the lack of MYI in the eastern part of the gate is replenished by FYI that is thinner than 1.5 m. In seasons 2010/2011 and 2016/2017, MYI fraction at the zonal gate is larger than in other years. In 2011/2012, from February to March, the indicated FYI is rather thick (> 2 m), similar to the indicated MYI towards the coast of Greenland.

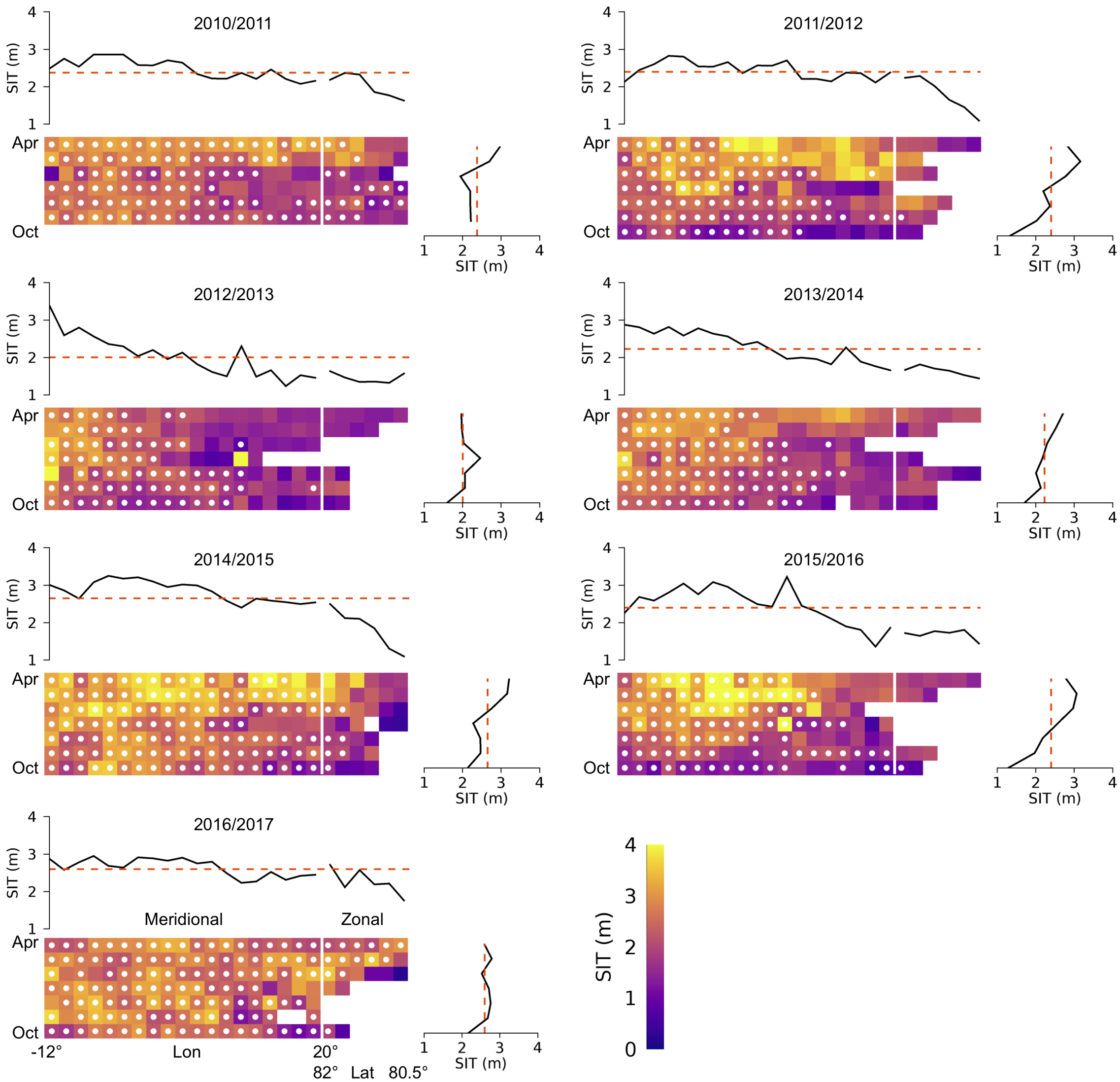

Figure 2. Spatiotemporal variability of sea ice thickness (SIT) at the Fram Strait gate from October to April between 2010 and 2017. Upper sub-panels show the temporal averaged SIT. Right sub-panels show the average over the gate SIT for each month within the October-April period. The white dots represent grid cells that contain multiyear ice.

Figure 3 shows the spatiotemporal distribution of the OSISAF ice drift along the meridional and zonal gates through each winter season. In contrast to ice thickness, the drift reveals a larger temporal variability with monthly differences of up to 10 km/d and without a distinct trend within each winter season. On the other hand, the OA period averages of the drift show a consistent spatial trend for all years, from less than 5 km/d in the east (20°E) and at the zonal gate, to a maximum of 9-10 km/d at about 6°W, followed by a decrease towards the coast of Greenland. The stationary peak at about 6°W suggests a large

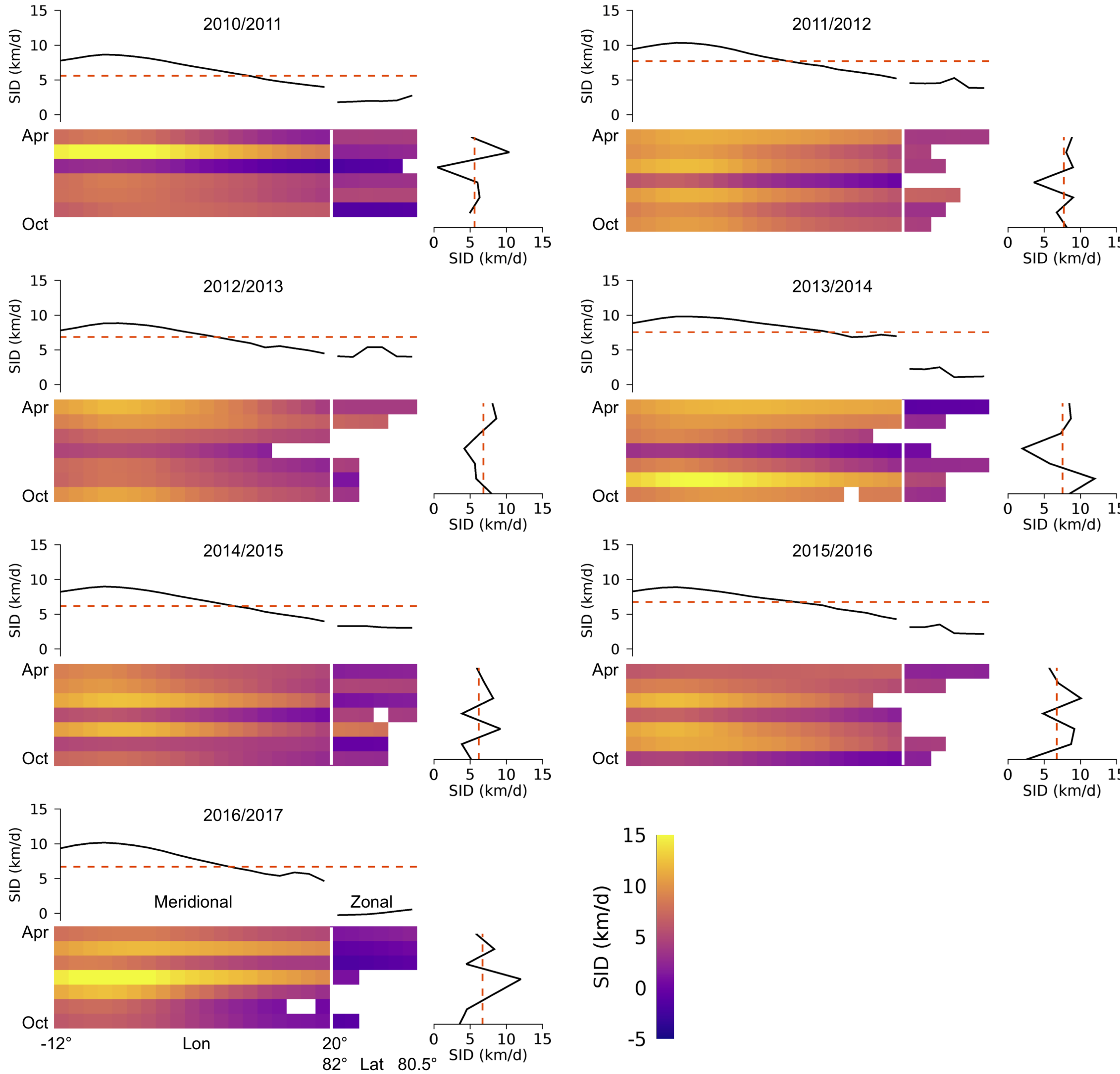

Figure 3. Spatiotemporal variability of OSISAF sea ice drift (SID) at the Fram Strait gate from October to April between 2010 and 2017. Upper sub-panels show the temporal average SID. Right sub-panels show the average over the gate SID for each month within the October-April period.

scale forcing and could be associated with the East Greenland Current (Rudels et al., 2002; de Steur et al., 2009). We notice that mean drift across the zonal gate is only 35 % of the mean drift across the meridional gate. The IFREMER and NSIDC ice drift also exhibit similar patterns as OSISAF (not shown).

Figure 4 shows the spatiotemporal distribution of the ice concentration along the meridional and zonal gates through each winter season. Ice concentration at the meridional gate is persistently high and ranges between 70 % and 100 %, with few

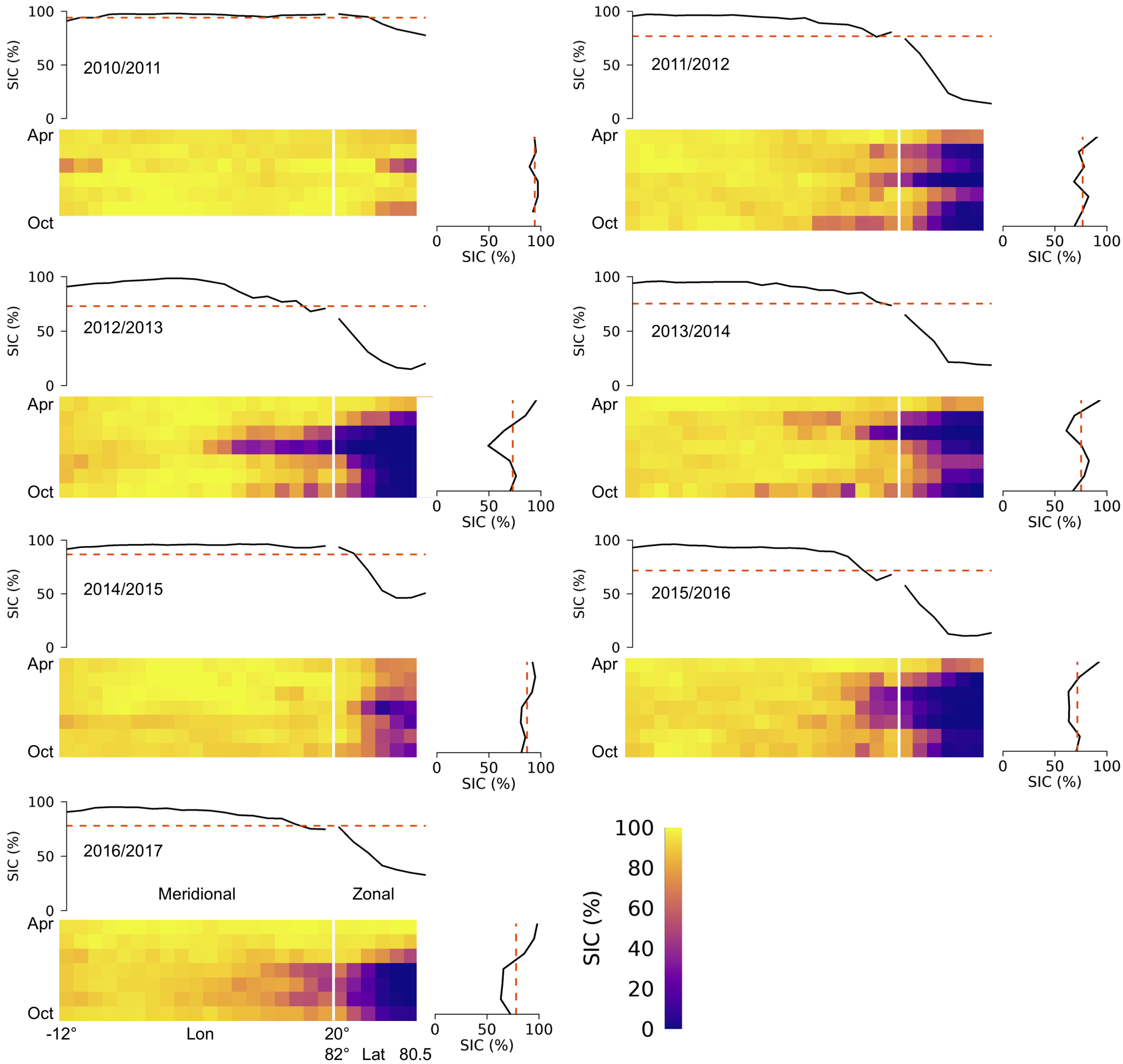

Figure 4. Spatiotemporal variability of OSISAF sea ice concentration (SIC) at the Fram Strait gate from October to April between 2010 and 2017. Upper sub-panels show the temporal average SIC. Right sub-panels show the average over the gate SIC for each month within the October-April period.

exceptions like January 2012/2013. In contrast, the zonal ice concentration shows higher variability, depending on the ice extent north of Svalbard, where the ocean remains ice free in some areas over several months.

Figure 5 illustrates ice drift, thickness, and concentration averaged over the entire gate and divided by their mean values to illustrate their variability and make it comparable. Here, ice concentration represents the fraction of ice covered area along the entire gate, including the zonal and meridional parts. As indicated in Figure 2, in contrast to ice drift, ice thickness shows a trend in most of the winter seasons. The same holds for the ice concentration as ice extent at the zonal gate north of Svalbard

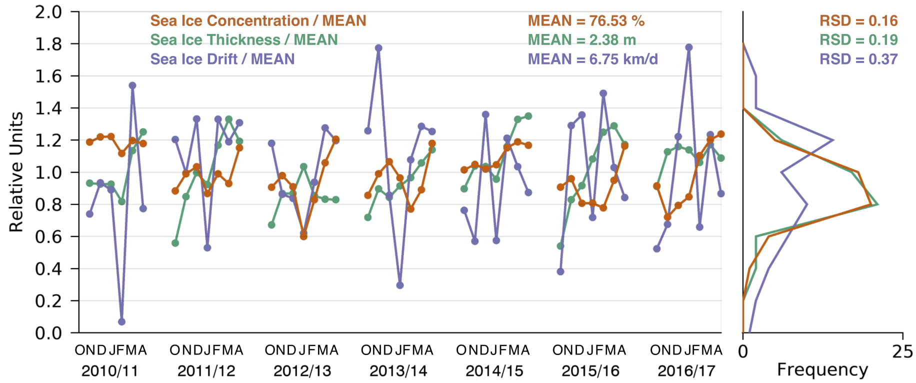

Figure 5. OSISAF sea ice drift, ice thickness, and ice concentration averaged over the entire Fram Strait gate, between October and April for winter seasons 2010/2011 to 2016/2017. Monthly values are divided by the mean of the data set for each parameter. The right box shows the corresponding histograms with the relative standard deviations (RSD).

Table 2. Monthly Arctic sea ice volume export through the Fram Strait in km^3/month, computed with OSISAF ice drift.

	Oct	Nov	Dec	Jan	Feb	Mar	Apr
2010/11	–	-227	-275	-267	-21	-540	-279
2011/12	-164	-214	-354	-129	-381	-379	-487
2012/13	-203	-182	-187	-103	-163	-299	-318
2013/14	-215	-400	-231	-78	-195	-345	-452
2014/15	-200	-165	-373	-160	-425	-429	-354
2015/16	-52	-261	-275	-177	-352	-348	-310
2016/17	-129	-151	-307	-466	-201	-431	-292

increases during winter in most of the seasons (Figure 4). In 2010/2011, the gate was almost entirely ice covered during the OA period. The histograms refer to the drift, thickness and concentration time series over the entire 7-years period. The drift distribution reveals two modes and a larger degree of dispersion than the ice thickness and concentration distribution. In order to compare and quantify the extent of variability of the three parameters we compute their relative standard deviation (RSD), which is the ratio of the standard deviation to the mean. We find that the RSD of the ice drift (0.37) is roughly double of the RSD of ice thickness (0.19) and ice concentration (0.16).

3.2 Sea ice volume flux and export through the Fram Strait

Figure 1 shows the retrieved ice volume flux as means over the OA period for the northern hemisphere for the 7 years of the CS2 operational period (2010-2017), using OSISAF ice drift data. The two major patterns are the Beaufort Gyre and the Transpolar Drift conveying ice towards Fram Strait. There, the ice fluxes reach maximum values of 20 km^3/month or more, with a steep

Table 3. Total Arctic sea ice volume export through the Fram Strait for winter seasons 2010/2011 - 2016/2017, added together over the November-April period. Volume export has been computed using three different ice drift products, using $Q_{\mathrm{Ex,OSISAF}}$ as the reference product. The last column shows the fraction of exported multiyear sea ice (% MYI).

Season	Q_{Ex} OSISAF ($10^3\mathrm{km}^3$)	ΔQ_{Ex} IFREMER-OSISAF	ΔQ_{Ex} NSIDC-OSISAF	MYI (%)
2010/11	-1.61 $\pm$ 0.21	+0.22	+0.15	90
2011/12	-1.94 $\pm$ 0.22	+0.48	+0.80	68
2012/13	-1.25 $\pm$ 0.16	+0.27	+0.36	64
2013/14	-1.70 $\pm$ 0.20	+0.36	+0.55	68
2014/15	-1.91 $\pm$ 0.23	+0.48	+0.38	92
2015/16	-1.72 $\pm$ 0.19	+0.53	+0.52	81
2016/17	-1.85 $\pm$ 0.21	+0.48		94

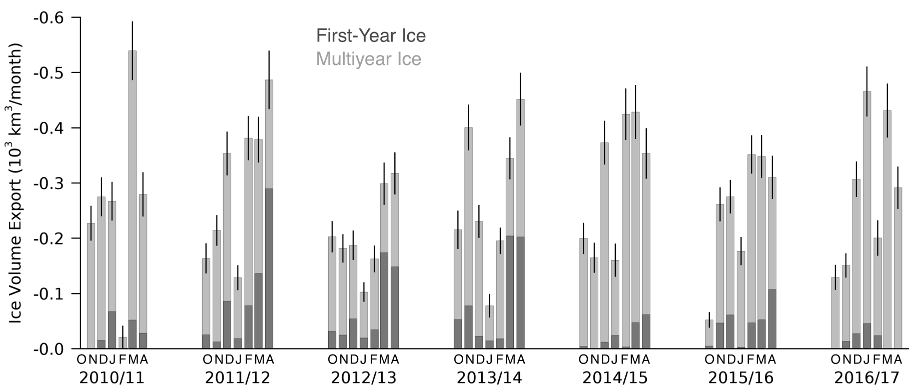

Figure 6. Monthly sea ice volume export through Fram Strait from October to April for the period 2010/2011 - 2016/2017, using the OSISAF ice drift product. The volume export is divided into first- and multiyear sea ice. Uncertainties are represented by error bars. October 2010 data are missing due to unavailability of CryoSat-2 data.

gradient along a north-south axis. The maximum values have to be considered in relation to the 25 km grid resolution and are likely different on smaller scales. MYI is mainly exported through the meridional part of the gate, while sea ice at the zonal part is primarily FYI. The monthly sea ice volume export through Fram Strait is shown in Table 2 and Figure 6. During the 7-years period, the maximum monthly ice volume export of -540 km^3/month occurs in March 2011, while the minimum of -21 km^3/month is found in February 2011. Table 3 provides the total ice volume export ($Q_{\mathrm{Ex,OSISAF}}$) through the Fram Strait gate for the NA period. We find a maximum export of -1910 $\pm$ 230 km^3 for 2011/2012 and a minimum of -1250 $\pm$ 160 km^3 in 2012/2013. The major fraction of exported sea ice is represented by MYI. However, in few months like April 2012, the fraction of exported FYI exceeds the MYI fraction. Table 3 shows the fraction of exported MYI averaged over the seasons. A maximum of 94 % occurs in 2016/2017 and a minimum of 64 % occurs in 2012/2013. The MYI fraction refers to grid cells which are indicated as MYI by using the ice type product.

3.3 Deriving sea ice volume export using different ice drift products

In order to investigate the impact of the chosen drift product on the volume export estimates, we compare ice volume flux through the Fram Strait gate using three different drift products. Figure 7a shows an example for monthly ice volume flux through the Fram Strait gate and the contributions to the meridional and zonal parts of the gate, using the three drift products. All three retrievals exhibit consistent temporal and spatial variations along the gate, but differ in magnitude. $Q_{\mathrm{Ex,OSISAF}}$ and $Q_{\mathrm{Ex,IFREMER}}$ always exceed $Q_{\mathrm{Ex,NSIDC}}$ by about 0.2-0.3 km^3/day. Uncertainties of the ice flux through each grid cell are in the range of 0.1 km^3/day. Figure 7b shows the monthly and seasonal ice volume export through the Fram Strait during the NA period between 2010 and 2017, computed with the three different drift products. The variations of $Q_{\mathrm{Ex,OSISAF}}$ and $Q_{\mathrm{Ex,IFREMER}}$ correlate, but differ in magnitude. Table 3 provides the corresponding annual differences between the products. Using IFREMER ice drift, the derived ice export is 200-500 km^3 lower than export derived using OSISAF ice drift, which corresponds to a mean difference of about -23 %. $Q_{\mathrm{Ex,NSIDC}}$ is the lowest among the three estimates and shows mean difference of about -26 %, relating to $Q_{\mathrm{Ex,OSISAF}}$. Also, the interannual changes of $Q_{\mathrm{Ex,NSIDC}}$ compared to both $Q_{\mathrm{Ex,OSISAF}}$ and $Q_{\mathrm{Ex,IFREMER}}$ are slightly different as $Q_{\mathrm{Ex,NSIDC}}$ decreases from 2010/2011 to 2011/2012, while the other both retrievals show an increase. In 2011/2012, the monthly difference of $Q_{\mathrm{Ex,NSIDC}}$ to the other retrievals is significantly higher than in other winter seasons, but the reason for this is unclear. Nevertheless, the main variations and the magnitudes of spatial gradients are similar for all products. Considering the correlation coefficients (r) between the monthly volume export retrievals (Figure 7b, upper panel), we find r($Q_{\mathrm{Ex,OSISAF}}$, $Q_{\mathrm{Ex,IFREMER}}$) = 0.94, r($Q_{\mathrm{Ex,OSISAF}}$, $Q_{\mathrm{Ex,NSIDC}}$) = 0.92 and $Q_{\mathrm{Ex,NSIDC}}$) = 0.90. Therefore, the choice of the drift products has no major impact on our export variability analysis. We also note, that it is not within the scope of this work to determine which product provides the most accurate estimate of sea ice drift in the Fram Strait.

4 Discussion

4.1 Relative contribution of sea ice drift, thickness and concentration to the volume flux variability

In order to understand the mechanisms behind the variability in ice volume export, we now examine the three input parameters, ice drift, thickness and concentration, in more detail. As shown in section 3.1, the thickness averaged across Fram Strait exhibits significant interannual changes with an overall increase in spring. This increase at the gate from autumn to spring can be associated with the thermodynamic ice growth and deformation of FYI and thin second-year ice. For example, in 2011/2012 and 2013/2014, thickness of FYI grid cells rises from October to April (Figure 2). In contrast, in 2016/2017, the fraction of FYI passing the gate is only 6 %, and consequently, we do not observe significant changes in mean ice thickness during the OA period. Similarly, we observe an increase in mean ice concentration at the gate during the OA period. Considering the ice drift, we find opposite features. The mean monthly drift in the time domain is highly variable, without a distinct trend over

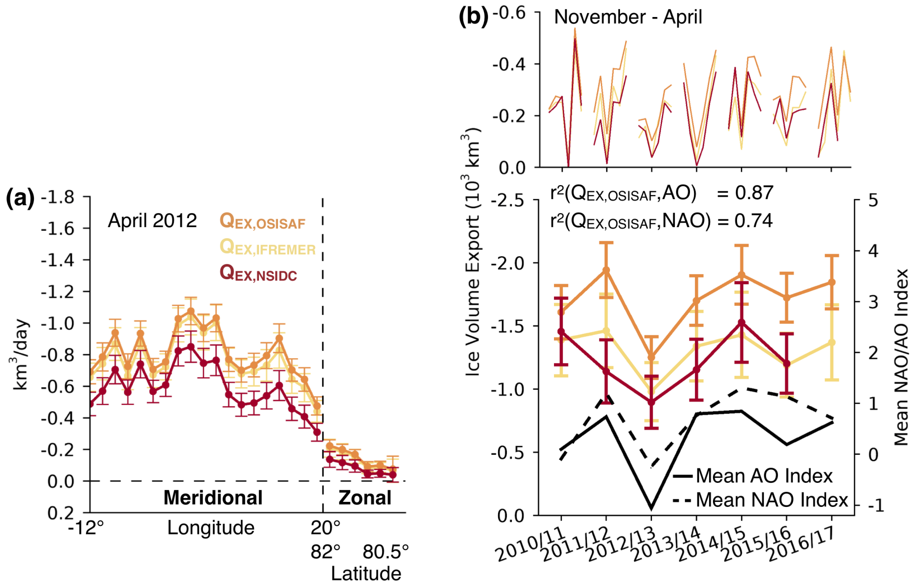

Figure 7. (a) Example for monthly ice volume export through the Fram Strait gate (April 2012) derived from three different ice drift products. (b) Monthly sea ice volume export (upper panel), and total Arctic sea ice volume export through the Fram Strait for winter seasons 2010/2011 - 2016/2017, added together over the November-April period and derived from three different ice drift products (lower panel). Mean Arctic Oscillation (AO) Index and mean North Atlantic Oscillation Index (NAO) are shown for the same period, including coefficients of determination (r^2).

the OA period (Figure 8a). These characteristics of the variability of input parameters affect the mean monthly ice volume export (Figure 8b). The mean seasonal cycle over the period 2010-2017 is characterized by minimums in October and January and the maximum in March. Considering seasonal cycles of drift, thickness, and concentration at the gate and comparing it with the seasonal cycle of the ice export, we find that the variability is mostly explained by the ice drift (Figure 8a) as also suggested by the RSD. On the other hand, the positive gradient of the ice volume export between autumn and spring with the annual maximum in March can be associated with the seasonal cycle of sea ice thickness (Figure 8a). This seems primarily driven by thermodynamic ice growth and deformation. Although the seasonal cycle of mean ice concentration along the entire gate shows positive gradients as well, with a similar RSD as the ice thickness, it seems to play a minor role for the ice export variability. This is because ice concentration variability at the meridional gate is small due to the persistent ice coverage over the season. Considered separately, we find a RSD of 0.78 at the zonal gate and a RSD of 0.08 at the meridional gate. But due to the smaller size, lower ice drift and thinner ice, the zonal volume flux is only about 4 % of the total ice export over the 7-years period.

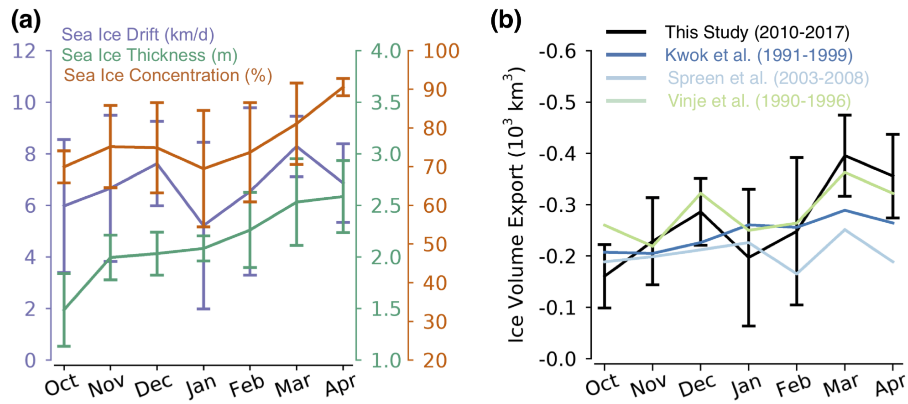

Figure 8. (a) Mean monthly sea ice drift, thickness and concentration at the Fram Strait gate over the years 2010/2011 - 2016/2017 with corresponding standard deviations. (b) Mean monthly ice volume export through the Fram Strait from this study, and from Spreen et al. (2009), Kwok et al. (2004), and Vinje et al. (1998) covering different periods.

4.2 Comparison to previous studies

sea ice export through the Fram Strait and its variability has been the focus of several previous studies. A major difference in the method is the choice of the position of the gate. Smedsrud et al. (2017) placed the gate at 79°N, Spreen et al. (2009) placed their most northern gate at 80°N, and Kwok and Rothrock (1999) placed their gate at about 81°N. Except for the study of Krumpen et al. (2016), all these previous studies use only a meridional gate or a straight connection between Greenland and Spitsbergen. The major advantage of using a gate positioned further north like at 82°N is that ice motion products and thickness estimates from satellites show lower uncertainties at this latitude. Indeed, errors and biases of low resolution ice drift data derived from passive microwave and scatterometer data become larger as ice velocity increases, and velocity tends to be larger with steeper gradients south of 82°N (Sumata et al., 2014, 2015). In addition, uncertainty of CS2 ice thickness increases at lower latitudes, especially in Fram Strait due to sparse orbit coverage (Ricker et al., 2014, 2017b). Therefore, we followed the approach of Krumpen et al. (2016), placing the gate at 82°N, which appears to be a good choice in order to reduce uncertainty associated with our ice volume export estimate.

Figure 8b shows the mean monthly winter export from October to April from this study, compared to previous estimates (Kwok et al., 2004; Spreen et al., 2009; Vinje et al., 1998). Vinje et al. (1998) and Kwok et al. (2004) use upward-looking sonar (ULS) data for the estimation of ice thickness in the Fram Strait. Vinje et al. (1998) use ULS ice draft measurements from 1990-1996 in combination with buoy and SAR-based ice drift estimates, and estimate ice volume fluxes through the Fram Strait that show maxima of up to about -600 km^3/month. Kwok et al. (2004) investigated nearly the same period (1991-1999) and find a maximum monthly export of -509 km^3/month in December 1994. Their estimates are generally lower than in Vinje et al. (1998). Spreen et al. (2009) use ice thickness and drift estimates derived from satellite data to compute ice volume flux, and therefore, their study is methodically similar to our work. However, besides the different gate at 80°N, they use a different ice thickness retrieval (ICESat) and another low resolution ice drift data set (Cersat/Ifremer, AMSR-E) to derive ice volume export. For the period 2003-2008, they estimate monthly winter ice volume export ranging from -100 to -420 km^3/month, using ULS ice thickness estimates to complement the two month-long ICESat measurement periods per year. The largest difference of about 150 km^3 between the lowest and largest estimate is found in March. Our estimate seems to be the one with the highest change between October and April, e.g. our estimates are the lowest in October, and the highest in April (Figure 8b). Our seasonal cycle also reveals higher variability. Several factors might cause this discrepancy:

1. The observing periods are not overlapping and therefore, differences in mean monthly export can be caused by natural variations in ice thickness and drift.

2. Bottom melt due to the recirculation of warm Atlantic water between between 82°N and 80°N might lead to a reduction in ice volume (Wekerle et al., 2017).

3. The low resolution of the drift data might lead to systematic uncertainties in the volume flux at the gate, especially near the coast and the ice margins, affecting all retrievals.

4. Systematic differences between the CS2 and ICESat ice thickness retrievals may appear because of different retrieval algorithms and different sensor characteristics.

5. Ice drift at 80°N might be underestimated due large ice velocities, which are not well captured in radiometer- and scatterometer-based drift products.

Despite these differences, estimates from different studies exhibit consistent features, such as the maximum in March. In the following, we will discuss the interannual variability and the role of atmospheric circulation patterns.

4.3 Interannual ice volume export variability

The time series of winter ice volume export through the Fram Strait reveals a significant decrease of 500 km^3 from 2011/2012 to 2012/2013 (Figure 7). This decrease is characterized by a drop of both the mean ice drift and the thickness through Fram Strait. Comparing the pan Arctic ice condition in both winters, a decrease of ice thickness north of Fram Strait has been reported for 2012/2013 by Ricker et al. (2017a), and was found to be mainly a result of anomalous summer melt and late freeze up in 2012. The ice in the area north of Fram Strait is the main source of exported ice (Smedsrud et al., 2017) and thus, we also find a drop in ice thickness at the Fram Strait for 2012/2013, which is accompanied by a lower mean drift (Figure 5). In contrast, in winter season 2013/2014, which followed a cold Arctic summer with low melt rates (Tilling et al., 2015), ice thickness at the gate is increasing, accompanied by a higher mean drift (Figure 5). This results in an ice volume export comparable to 2010/2011 (Figure 7).

We also examine the link between ice volume export and North Atlantic Oscillation (NAO) index and the Arctic Oscillation (AO) index (Figure 7b). The NAO index is defined as the sea level pressure anomaly between Lisbon, Portugal, and Reykjavik, Iceland. A positive NAO index is associated with an Icelandic low and a corresponding high-pressure system over the Azores.

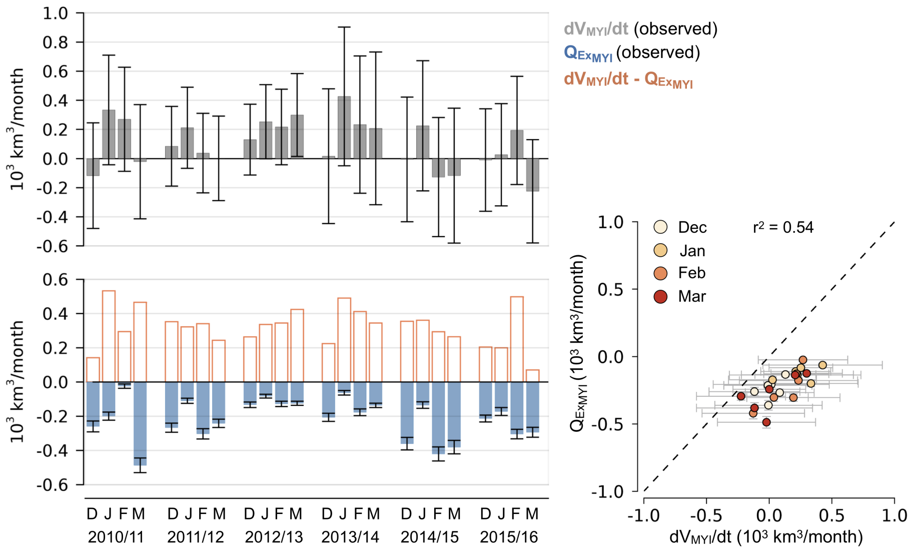

Figure 9. Monthly MYI volume export through the Fram Strait ($Q_{\mathrm{Ex_{MYI}}}$) and simultaneous Arctic MYI volume growth rates (dV_{MYI}/dt) between December and March for the winter seasons 2010/2011 - 2015/2016. Error bars represent the corresponding uncertainties. The scattergram shows the relation between dV_{MYI}/dt and $Q_{\mathrm{Ex_{MYI}}}$, and corresponding coefficient of determination (r^2).

When the Icelandic low is intensified, the sea level pressure gradient in the Fram Strait increases, leading to strong northerly winds and hence, increased sea ice drift (Kwok and Rothrock, 1999; Kwok et al., 2013; Ionita et al., 2016; Smedsrud et al., 2017). Thus, a high, positive NAO index is associated with high ice volume export rates, since ice drift primarily drives the ice volume export variability. If both pressure systems are weak or even reversed, the NAO phase becomes negative and correlation between NAO and sea level pressure gradient along the Fram Strait decreases. The variability of the NAO is largest during the winter season. We have obtained monthly NAO indices from the National Oceanic and Atmospheric Administration (NOAA) and averaged them over the NA period. Positive phases (>1) of the NAO index occurred in 2011/2012 and 2014/2015, coinciding with increased mean monthly ice volume export rates (Figure 7b).

The sea level pressure gradient variability through the Fram Strait is also captured in the AO and its corresponding index, described in Thompson and Wallace (1998). The AO pattern involves an oscillation of the sea level pressure between the Arctic basin and the surrounding zonal belt. The AO therefore includes characteristics of the NAO, which is regionally bounded. We have obtained monthly AO indices from NOAA (http://www.cpc.ncep.noaa.gov) and averaged them over the NA period. The variability of the AO index is similar to the variability of the NAO index and the ice volume export, especially if the flux is computed with IFREMER and OSISAF ice drift (Figure 7b). The correlation between ice export and AO index (r^2 = 0.87) is larger than with the NAO index (r^2 = 0.74). This is because the NAO index decreases is 2016/2017, while the ice volume export increases compared to the previous year. However, we acknowledge that a longer time series is required to obtain statistical meaningful correlation coefficients.

4.4 The impact of ice volume export on Arctic ice mass balance

Kwok et al. (1999) investigated the area balance of the Arctic Ocean perennial ice zone between October 1996 and April 1997. Using RADARSAT data, they reported that winter MYI area loss can be explained almost entirely by ice export. Moreover, their findings suggest that export is dominated by ice flux through the Fram Strait, while export through other gates like Nares Strait plays a minor role. According to Kwok et al. (1999), MYI area export through Nares Strait is about 5 % of the Fram Strait MYI area export. The balance of MYI area is only affected by export and ice dynamics, assuming that the net melt of MYI area is zero in winter. As a consequence, Arctic MYI area is decreasing from October to April, and in turn, this decrease is almost entirely balanced by exported MYI area (Kwok et al., 1999).

In the following, we investigate the ice volume balance of the Arctic MYI. In contrast to MYI area, we assume that MYI volume growth rate of the Arctic Ocean domain (dV_{MYI}/dt) is affected by both export ($Q_{\mathrm{Ex_{MYI}}}$) and ice volume gain due to thermodynamic growth ($dV_{\mathrm{therm_{MYI}}}/dt$). Neglecting net melt of MYI in winter, we can write:

$$\frac{dV_{\mathrm{MYI}}}{dt} = Q_{\mathrm{Ex_{MYI}}} + \left(\frac{dV_{\mathrm{therm_{MYI}}}}{dt} + \frac{dV_{\mathrm{resid_{MYI}}}}{dt}\right). \tag{9}$$

The term $dV_{\mathrm{resid_{MYI}}}/dt$ accounts for residual contributions. This includes ice deformation that might change the bulk ice density, which we assume to be constant. Moreover, new forming openings within the MYI zone due to divergence can bias the ice type classification when such areas are erroneously classified as MYI. This effect leads to a positive bias of dV_{MYI}/dt. A quantitative separation between $dV_{\mathrm{resid_{MYI}}}/dt$ and $dV_{\mathrm{therm_{MYI}}}/dt$ is difficult. Therefore, we only consider the entire contribution of the second term in Eq. (9).

We estimate monthly Arctic MYI volume growth dV_{MYI}/dt by a 3-point Lagrangian interpolation scheme, where we exclude all ice south of the Fram Strait gate. Since CS2 ice thickness data are not available in October 2010, we compute dV_{MYI}/dt using data over the NA period and therefore obtain dV_{MYI}/dt values for December to March. Figure 9 shows monthly dV_{MYI}/dt and corresponding $Q_{\mathrm{Ex_{MYI}}}$ for 6 years. In addition, it shows the residual ($dV_{\mathrm{resid_{MYI}}}/dt + dV_{\mathrm{therm_{MYI}}}/dt$), which is not directly observed, but deduced by subtracting $Q_{\mathrm{Ex_{MYI}}}$ from dV_{MYI}/dt. Winter season 2016/2017 is excluded here due to erroneous MYI ice classification, which affects dV_{MYI}/dt and $Q_{\mathrm{Ex_{MYI}}}$ (Section 2.3).

MYI volume growth dV_{MYI}/dt does not follow a seasonal cycle as it is the case for FYI volume growth that is primarily driven by the thermodynamic ice growth (Ricker et al., 2017a). It appears that $Q_{\mathrm{Ex_{MYI}}}$ is just in the range to almost or entirely balance the volume gain of the second term in Eq. (9), ($dV_{\mathrm{resid_{MYI}}}/dt$ + $dV_{\mathrm{therm_{MYI}}}/dt$). For example, in 2014/2015 and 2015/2016, mean dV_{MYI}/dt is nearly zero due to large $Q_{\mathrm{Ex_{MYI}}}$ between December and March. It is possible that $Q_{\mathrm{Ex_{MYI}}}$ exceeds $dV_{\mathrm{therm_{MYI}}}/dt$, leading to a net reduction of Arctic MYI volume when considering a positive bias due to erroneous MYI type classification. However, the variability of dV_{MYI}/dt is significantly driven by $Q_{\mathrm{Ex_{MYI}}}$, revealing a coefficient of determination (r^2) of 0.54, which means that 54 % of dV_{MYI}/dt during winter can be explained by variations of $Q_{\mathrm{Ex_{MYI}}}$, assuming a linear relationship. From that, we can deduce that the variability of dV_{MYI}/dt is significantly driven by the variability of the ice drift in the Fram Strait.

The high correlation (0.74) between $Q_{\mathrm{Ex_{MYI}}}$ and dV_{MYI}/dt is also noticeable. This proves the accuracy of Arctic MYI volume estimates as the correlation between $Q_{\mathrm{Ex_{MYI}}}$ and dV_{MYI}/dt exposes the signal of ice volume export in the MYI volume budget. In case of large errors in dV_{MYI}/dt as indicated in Figure 9 by the error bars, correlation with $Q_{\mathrm{Ex}_{\mathrm{MYI}}}$ would be degraded.

5 Conclusions

Here we have used, for the first time, the CryoSat-2 ice thickness retrievals in order to quantify the sea ice export through Fram Strait. We performed a detailed analysis of variability and important processes for the Arctic multiyear ice (MYI) mass balance. Based on our analysis, the following conclusions can be drawn:

1. Based on different ice drift products, the three ice volume export retrievals ($Q_{\mathrm{Ex,OSISAF}}$, $Q_{\mathrm{Ex,IFREMER}}$, $Q_{\mathrm{Ex,NSIDC}}$) exhibit similarities in their variability (correlations r>0.9), although they differ in magnitude by -23 % ($Q_{\mathrm{Ex,IFREMER}}$) and -26 % ($Q_{\mathrm{Ex,NSIDC}}$), compared to $Q_{\mathrm{Ex,OSISAF}}$. In order to investigate long-term trends in ice volume export derived from multiple satellite observations, we therefore need to construct multi-sensor consistent time series of ice drift, thickness, and concentration. Moreover, a consistent methodology to compute ice volume flux through Fram Strait is required.

2. Ice drift shows coherent spatial variability across Fram Strait, but high frequency variability from month to month. The mean monthly ice drift across Fram Strait shows a peak at about 6°W, which could be associated with the East Greenland Current.

3. The relative standard deviation (RSD) is a measure to compare the variability of different physical quantities. At the Fram Strait gate, RSD of ice drift (0.37) is roughly twice as high as the RSD of ice thickness (0.19) and concentration (0.16) for the observation period of 2010/2011-2016/1017, revealing that ice drift is the main driver of seasonal and interannual variability of ice volume export. However, the seasonal trend of ice volume export is driven by variations in ice thickness due to the thermodynamic growth that typically leads to a maximum in March. Ice concentration variability is large at the zonal gate (RSD = 0.78), but small at the meridional gate (RSD = 0.08), where 96 % of the sea ice is exported.

4. Monthly sea-ice volume export through Fram Strait varies between -21 and -540 km^3/month.

5. The interannual variations of ice volume export can be explained by large scale variability of the atmospheric circulation captured by the Arctic Oscillation ($r^2 = 0.87$) and North Atlantic Oscillation indices ($r^2 = 0.74$).

6. While the seasonal cycle of Arctic first-year ice volume is driven by thermodynamic ice growth, 54 % of the changes in Arctic MYI volume over the December-March period can be explained by ice volume export through the Fram Strait.

Data availability. Sea ice concentration, sea ice type and sea ice drift data are provided by OSISAF (http://osisaf.met.no). CryoSat-2 ice thickness data from 2010-2017 are provided by http://www.meereisportal.de. IFREMER ice drift data from 2010 to 2017 are provided via CERSAT (http://cersat.ifremer.fr). NSIDC ice drift data from 2010 to 2015 are provided via https://nsidc.org.

Author contributions. Robert Ricker conducted the ice volume flux calculations and the analysis. Fanny Girard-Ardhuin, Thomas Krumpen and Camille Lique contributed to the analysis of the ice volume flux data. Robert Ricker wrote the paper and all Co-authors contributed to the discussion and gave input for writing.

Competing interests. The authors declare no conflict of interest.

Acknowledgements. This work has been conducted in the framework of the project: Space-borne observations for detecting and forecasting sea ice cover extremes (SPICES) funded by the European Union (H2020) (Grant: 640161). CryoSat-2 data are provided by http://www.meereisportal.de (Grant REKLIM-2013-04). Moreover, this work was supported by the German Ministry for Science and Education under Grant 03F0777A (QUARCCS) and the CORESAT project funded by the Norwegian Research Council (grant 222681).

References

Aaboe, S., Breivik, L.-A., Sørensen, A., Eastwood, S., and Lavergne, T.: Global sea ice edge and type product user's manual, OSI-403-c & EUMETSAT, 2016.

Alexandrov, V., Sandven, S., Wahlin, J., and Johannessen, O. M.: The relation between sea ice thickness and freeboard in the Arctic, The Cryosphere, 4, 373–380, https://doi.org/10.5194/tc-4-373-2010, http://www.the-cryosphere.net/4/373/2010/, 2010.

Comiso, J. C.: Arctic multiyear ice classification and summer ice cover using passive microwave satellite data, Journal of Geophysical Research: Oceans, 95, 13 411–13 422, https://doi.org/10.1029/JC095iC08p13411, http://dx.doi.org/10.1029/JC095iC08p13411, 1990.

de Steur, L., Hansen, E., Gerdes, R., Karcher, M., Fahrbach, E., and Holfort, J.: Freshwater fluxes in the East Greenland Current: A decade of observations, Geophysical Research Letters, 36, https://doi.org/10.1029/2009GL041278, https://doi.org/10.1029/2009GL041278, 2009.

Dickson, R. R., Meincke, J., Malmberg, S.-A., and Lee, A. J.: The "great salinity anomaly" in the Northern North Atlantic 1968–1982, Progress in Oceanography, 20, 103 – 151, https://doi.org/https://doi.org/10.1016/0079-6611(88)90049-3, http://www.sciencedirect.com/science/article/pii/0079661188900493, 1988.

Eastwood, S.: OSI SAF Sea Ice Product Manual, v3.8 edn., http://osisaf.met.no, 2012.

Ezraty, R., Girard-Ardhuin, F., and Piollé, J.-F.: Sea ice drift in the central Arctic estimated from SeaWinds/QuikSCAT backscatter maps, User's Manual. Laboratoire d'Océanographie Spatiale(Département d'Océanographie Physique et Spatiale), IFREMER, Brest, 2007.

Girard-Ardhuin, F. and Ezraty, R.: Enhanced Arctic Sea Ice Drift Estimation Merging Radiometer and Scatterometer Data, IEEE Transactions on Geoscience and Remote Sensing, 50, 2639–2648, https://doi.org/10.1109/TGRS.2012.2184124, ftp://ftp.ifremer.fr/ifremer/cersat/products/gridded/psi-drift/, 2012.

Helm, V., Humbert, A., and Miller, H.: Elevation and elevation change of Greenland and Antarctica derived from CryoSat-2, The Cryosphere, 8, 1539–1559, https://doi.org/10.5194/tc-8-1539-2014, http://www.the-cryosphere.net/8/1539/2014/, 2014.

Hendricks, S., Ricker, R., and Helm, V.: User Guide - AWI CryoSat-2 Sea Ice Thickness Data Product (v1.2), hdl:10013/epic.48201, 2016.

Holland, M. M., Bitz, C. M., and Tremblay, B.: Future abrupt reductions in the summer Arctic sea ice, Geophysical Research Letters, 33, https://doi.org/10.1029/2006GL028024, http://dx.doi.org/10.1029/2006GL028024, 2006.

Ionita, M., Scholz, P., Lohmann, G., Dima, M., and Prange, M.: Linkages between atmospheric blocking, sea ice export through Fram Strait and the Atlantic Meridional Overturning Circulation, Scientific Reports, 6, 32 881 EP –, http://dx.doi.org/10.1038/srep32881, 2016.

Ivanova, N., Johannessen, O. M., Pedersen, L. T., and Tonboe, R. T.: Retrieval of Arctic Sea Ice Parameters by Satellite Passive Microwave Sensors: A Comparison of Eleven Sea Ice Concentration Algorithms, IEEE Transactions on Geoscience and Remote Sensing, 52, 7233–7246, https://doi.org/10.1109/TGRS.2014.2310136, 2014.

Krumpen, T., Gerdes, R., Haas, C., Hendricks, S., Herber, A., Selyuzhenok, V., Smedsrud, L., and Spreen, G.: Recent summer sea ice thickness surveys in Fram Strait and associated ice volume fluxes, The Cryosphere, 10, 523–534, https://doi.org/10.5194/tc-10-523-2016, http://www.the-cryosphere.net/10/523/2016/, 2016.

Kwok, R.: Near zero replenishment of the Arctic multiyear sea ice cover at the end of 2005 summer, Geophysical Research Letters, 34, https://doi.org/10.1029/2006GL028737, http://dx.doi.org/10.1029/2006GL028737, 2007.

Kwok, R. and Cunningham, G.: Variability of Arctic sea ice thickness and volume from CryoSat-2, Philosophical Transactions of the Royal Society of London A: Mathematical, Physical and Engineering Sciences, 373, 20140 157, 2015.

Kwok, R. and Rothrock, D. A.: Variability of Fram Strait ice flux and North Atlantic Oscillation, Journal of Geophysical Research: Oceans, 104, 5177–5189, https://doi.org/10.1029/1998JC900103, http://dx.doi.org/10.1029/1998JC900103, 1999.

Kwok, R., Cunningham, G. F., and Yueh, S.: Area balance of the Arctic Ocean perennial ice zone: October 1996 to April 1997, Journal of Geophysical Research: Oceans, 104, 25 747–25 759, https://doi.org/10.1029/1999JC900234, http://dx.doi.org/10.1029/1999JC900234, 1999.

Kwok, R., Cunningham, G. F., and Pang, S. S.: Fram Strait sea ice outflow, Journal of Geophysical Research: Oceans, 109, n/a–n/a, https://doi.org/10.1029/2003JC001785, http://dx.doi.org/10.1029/2003JC001785, c01009, 2004.

Kwok, R., Spreen, G., and Pang, S.: Arctic sea ice circulation and drift speed: Decadal trends and ocean currents, Journal of Geophysical Research: Oceans, 118, 2408–2425, https://doi.org/10.1002/jgrc.20191, https://agupubs.onlinelibrary.wiley.com/doi/abs/10.1002/jgrc.20191, 2013.

Lavergne, T., Eastwood, S., Teffah, Z., Schyberg, H., and Breivik, L.-A.: Sea ice motion from low-resolution satellite sensors: An alternative method and its validation in the Arctic, Journal of Geophysical Research: Oceans, 115, n/a–n/a, https://doi.org/10.1029/2009JC005958, http://dx.doi.org/10.1029/2009JC005958, c10032, 2010.

Laxon, S., Peacock, N., and Smith, D.: High interannual variability of sea ice thickness in the Arctic region, Nature, 425, 947–950, 2003.

Laxon, S. W., Giles, K. A., Ridout, A. L., Wingham, D. J., Willatt, R., Cullen, R., Kwok, R., Schweiger, A., Zhang, J., Haas, C., Hendricks, S., Krishfield, R., Kurtz, N., Farrell, S., and Davidson, M.: CryoSat-2 estimates of Arctic sea ice thickness and volume, Geophysical Research Letters, 40, 732–737, https://doi.org/10.1002/grl.50193, http://dx.doi.org/10.1002/grl.50193, 2013.

Lique, C., Treguier, A. M., Scheinert, M., and Penduff, T.: A model-based study of ice and freshwater transport variability along both sides of Greenland, Climate Dynamics, 33, 685–705, https://doi.org/10.1007/s00382-008-0510-7, https://doi.org/10.1007/s00382-008-0510-7, 2009.

Maslanik, J., Stroeve, J., Fowler, C., and Emery, W.: Distribution and trends in Arctic sea ice age through spring 2011, Geophysical Research Letters, 38, https://doi.org/10.1029/2011GL047735, http://dx.doi.org/10.1029/2011GL047735, 2011.

Parkinson, C. L. and Comiso, J. C.: On the 2012 record low Arctic sea ice cover: Combined impact of preconditioning and an August storm, Geophysical Research Letters, 40, 1356–1361, https://doi.org/10.1002/grl.50349, http://dx.doi.org/10.1002/grl.50349, 2013.

Ricker, R., Hendricks, S., Helm, V., Skourup, H., and Davidson, M.: Sensitivity of CryoSat-2 Arctic sea-ice freeboard and thickness on radar-waveform interpretation, The Cryosphere, 8, 1607–1622, https://doi.org/10.5194/tc-8-1607-2014, http://www.the-cryosphere.net/8/1607/2014/, 2014.

Ricker, R., Hendricks, S., Girard-Ardhuin, F., Kaleschke, L., Lique, C., Tian-Kunze, X., Nicolaus, M., and Krumpen, T.: Satellite-observed drop of Arctic sea ice growth in winter 2015–2016, Geophysical Research Letters, 44, 3236–3245, https://doi.org/10.1002/2016GL072244, http://dx.doi.org/10.1002/2016GL072244, 2016GL072244, 2017a.

Ricker, R., Hendricks, S., Kaleschke, L., Tian-Kunze, X., King, J., and Haas, C.: A weekly Arctic sea-ice thickness data record from merged CryoSat-2 and SMOS satellite data, The Cryosphere, 11, 1607–1623, https://doi.org/10.5194/tc-11-1607-2017, https://www.the-cryosphere.net/11/1607/2017/, 2017b.

Rudels, B., Fahrbach, E., Meincke, J., Budéus, G., and Eriksson, P.: The East Greenland Current and its contribution to the Denmark Strait overflow, ICES Journal of Marine Science, 59, 1133–1154, https://doi.org/10.1006/jmsc.2002.1284, +http://dx.doi.org/10.1006/jmsc.2002.1284, 2002.

Smedsrud, L. H., Halvorsen, M. H., Stroeve, J. C., Zhang, R., and Kloster, K.: Fram Strait sea ice export variability and September Arctic sea ice extent over the last 80 years, The Cryosphere, 11, 65–79, https://doi.org/10.5194/tc-11-65-2017, https://www.the-cryosphere.net/11/65/2017/, 2017.

Spreen, G., Kern, S., Stammer, D., and Hansen, E.: Fram Strait sea ice volume export estimated between 2003 and 2008 from satellite data, Geophysical Research Letters, 36, n/a–n/a, https://doi.org/10.1029/2009GL039591, http://dx.doi.org/10.1029/2009GL039591, l19502, 2009.

Spreen, G., Kwok, R., and Menemenlis, D.: Trends in Arctic sea ice drift and role of wind forcing: 1992–2009, Geophysical Research Letters, 38, https://doi.org/10.1029/2011GL048970, http://dx.doi.org/10.1029/2011GL048970, l19501, 2011.

Stroeve, J. C., Markus, T., Boisvert, L., Miller, J., and Barrett, A.: Changes in Arctic melt season and implications for sea ice loss, Geophysical Research Letters, 41, 1216–1225, https://doi.org/10.1002/2013GL058951, http://dx.doi.org/10.1002/2013GL058951, 2013GL058951, 2014.

Sumata, H., Lavergne, T., Girard-Ardhuin, F., Kimura, N., Tschudi, M. A., Kauker, F., Karcher, M., and Gerdes, R.: An intercomparison of Arctic ice drift products to deduce uncertainty estimates, Journal of Geophysical Research: Oceans, 119, 4887–4921, https://doi.org/10.1002/2013JC009724, http://dx.doi.org/10.1002/2013JC009724, 2014.

Sumata, H., Gerdes, R., Kauker, F., and Karcher, M.: Empirical error functions for monthly mean Arctic sea-ice drift, Journal of Geophysical Research: Oceans, 120, 7450–7475, https://doi.org/10.1002/2015JC011151, http://dx.doi.org/10.1002/2015JC011151, 2015.

Thomas, D. R. and Rothrock, D. A.: The Arctic Ocean ice balance: A Kalman smoother estimate, Journal of Geophysical Research: Oceans, 98, 10 053–10 067, https://doi.org/10.1029/93JC00139, http://dx.doi.org/10.1029/93JC00139, 1993.

Thompson, D. W. J. and Wallace, J. M.: The Arctic oscillation signature in the wintertime geopotential height and temperature fields, Geophysical Research Letters, 25, 1297–1300, https://doi.org/10.1029/98GL00950, http://dx.doi.org/10.1029/98GL00950, 1998.

Tilling, R. L., Ridout, A., Shepherd, A., and Wingham, D. J.: Increased Arctic sea ice volume after anomalously low melting in 2013, Nature Geoscience, 8, 643–646, 2015.

Tilling, R. L., Ridout, A., and Shepherd, A.: Near-real-time Arctic sea ice thickness and volume from CryoSat-2, The Cryosphere, 10, 2003–2012, https://doi.org/10.5194/tc-10-2003-2016, http://www.the-cryosphere.net/10/2003/2016/, 2016.

Tonboe, R., Lavelle, J., Pfeiffer, R.-H., and Howe, E.: Product User Manual for OSI SAF Global Sea Ice Concentration, OSI-401-b & EUMETSAT, 2017.

Vinje, T., Nordlund, N., and Kvambekk, Å.: Monitoring ice thickness in Fram Strait, Journal of Geophysical Research: Oceans, 103, 10 437–10 449, https://doi.org/10.1029/97JC03360, http://dx.doi.org/10.1029/97JC03360, 1998.

Warren, S. G., Rigor, I. G., Untersteiner, N., Radionov, V. F., Bryazgin, N. N., Aleksandrov, Y. I., and Colony, R.: Snow depth on Arctic sea ice, Journal of Climate, 12, 1814–1829, 1999.

Wekerle, C., Wang, Q., Danilov, S., Schourup-Kristensen, V., von Appen, W.-J., and Jung, T.: Atlantic Water in the Nordic Seas: Locally eddy-permitting ocean simulation in a global setup, Journal of Geophysical Research: Oceans, 122, 914–940, https://doi.org/10.1002/2016JC012121, http://dx.doi.org/10.1002/2016JC012121, 2017.

Wingham, D., Francis, C., Baker, S., Bouzinac, C., Brockley, D., Cullen, R., de Chateau-Thierry, P., Laxon, S., Mallow, U., Mavrocordatos, C., Phalippou, L., Ratier, G., Rey, L., Rostan, F., Viau, P., and Wallis, D.: CryoSat: A mission to determine the fluctuations in Earth's land and marine ice fields, Advances in Space Research, 37, 841 – 871, https://doi.org/10.1016/j.asr.2005.07.027, 2006.